UNIVERSITATEA POLITEHNICA DIN BUCUREŞTI
Școala Doctorală Chimie Aplicată și Știința Materialelor
Departamentul Inginerie Chimică și Biochimică

UNIVERSITÉ CLAUDE BERNARD LYON 1
École Doctorale Interdisciplinaire Sciences - Santé
Laboratoire Ingénierie des Matériaux Polymères

ABSTRACT

MATHEMATICAL MODELLING OF THE CHITOSAN FIBER FORMATION BY WET-SPINNING

MODELAREA MATEMATICĂ A FORMĂRII FIBRELOR DE CHITOSAN PRIN FILARE UMEDĂ

MODELISATION DU PROCEDE D'ELABORATION DE FIBRES DE CHITOSANE

Doctorand: Ing. Alin Alexandru ENACHE

Conducători ştiinţifici: Prof. Grigore Bozga

Prof. Jean-Pierre Puaux

COMISIA DE DOCTORAT

Președinte	Prof. Dănuț- Ionel VĂIREANU	Universitatea Politehnica din București
Conducător de doctorat	Prof. Jean-Pierre PUAUX	Université Claude-Bernard Lyon 1
Conducător de doctorat	Prof. Grigore BOZGA	Universitatea Politehnica din București
Referent	Prof. Laurent DAVID	Université Claude-Bernard Lyon 1
Referent	Prof. Jacques FAGES	École Nationale Supérieure des Mines d'Albi-Carmaux (IMT Mines Albi)
Referent	Prof. Teodor TODINCĂ	Universitatea Politehnica din Timișoara
Referent	Conf. Gheorghe BUMBAC	Universitatea Politehnica din București

2018

TABLE OF CONTENTS

INTRODUCTION

Among the natural polymers, the chitosans are substances of high practical interest, combining a unique set of properties such as biocompatibility and biodegradability, antimicrobial activity, low immunogenicity and low toxicity. Since they are soluble in acidic aqueous media, chitosans can be processed in a variety of physical forms such as solutions, hydrogels, membranes or multimembrane hydrogels, micro and nanoparticles and finally solid forms as nanofibers, films, yarns, scaffolds lyophilizates, etc.

In the last decades there were published many studies regarding the practical uses of the chitosan, of which the medical ones predominate (such as drug and gene delivery, scaffold materials for tissue engineering in vivo or in vitro, skin regeneration, wound healing or cartilage repair). Many of these applications are based on the usage of chitosan in the physical state of gel (hydrogels). As will be shown, the chitosan gels are usually prepared by coagulation (gelation) of its aqueous solutions. The practice evidenced that the kinetics of the gelation step controls the gel properties, appearing the possibility to modulate the mechanical and biological properties of chitosan hydrogels by an appropriate modulation of the neutralization kinetics.

In practice, a convenient method for chitosan hydrogels preparation consists in the dissolution of a chitosan (with given degree of acetylation, and molar weight distribution) into an aqueous acid solution (e.g. acetic acid or hydrochloric acid), followed by a coagulation step, using a liquid or gaseous base as coagulation agent (sodium or potassium hydroxide solutions at various concentrations, ammonia solution or ammonia vapors etc.). This technique was found particularly adequate for wound dressing hydrogels or in the preparation of chitosan fibers.

The physical (e.g. transport), mechanical and biological (resorption rate and resorption mechanisms) properties of chitosan physical hydrogels are determined, for a large part, by the gelation conditions. Thus, a precise modeling of the gelation kinetics is essential for the design and property control of such hydrogels. The gelation is usually controlled by the diffusion of the coagulation agent through the formed hydrogel, even if the diffusion coefficients in hydrogel media, water and polyelectrolyte solutions are frequently hypothesized to be identical.

Very useful in the treatment of wounds are the chitosan fibers, that can be used as such, or woven as textile materials. Practically, the chitosan fibers are obtained by spinning of relatively concentrated and viscous solutions, most frequently by wet spinning. This technique is applicable when the Newtonian viscosity of aqueous or hydro-alcoholic chitosan solutions is high ($\eta_o > 900$ Pa·s), thus ensuring the ability to form continuous and stable gelated macro-filaments. Note that the method of melt spinning is not applicabe in the case of chitosan due to its thermal degradation.

The majority of the above presented utilizations suppose a preparation stage of the chitosan hydrogels from its solutions, by controlled neutralization. In the design of the coagulation processes, it was proved that an important factor is the coagulant transport inside the hydrogel's structure. This transport occurs predominantly by diffusion mechanism, which is expected to be influenced by the presence of the chitosan macromolecules in structure of the gel.

In spite of its practical importance, the diffusion inside the chitosan gels is poorly investigated. The main objective of this work was the investigation, by experiments and mathematical modelling, of the chitosan coagulation kinetics and particularly the coagulant diffusion in the chitosan hydrogels. In all the studies presented, there were considered chitosan hydrogels obtained from acid aqueous solutions, using the sodium hydroxide (NaOH) as coagulant.

The results of the experimental and theoretical investigations, on the chitosan coagulation and coagulant diffusion in chitosan hydrogels, were used in the study of the chitosan wet-spinning process. The experiments were carried out on a laboratory scale plant existing in the Polymer Engineering Laboratory, University Claude Bernard Lyon 1.

This thesis is structured in five chapters, an introduction section and a section presenting the general conclusions of the research.

In the **Chapter 1** is presented a literature review regarding the chitosan sources and its purification, the determination of the chitosan's physical properties and the chitosan's applications. Also, in this chapter are presented information and data regarding the gel preparation and properties, as well as the main methods of chitosan spinning. Finally, there are presented the main theories and models describing the mass transport by diffusion in hydrogels.

The **Chapter 2** presents the experimental techniques used in this work for characterization of chitosan (determination of the average molar weight, water content of chitosan, chitosan degree of acetylation), the method used for the chitosan hydrogels preparation in disk and cylindrical forms, as well as the techniques for chitosan hydrogels characterization (rheological analysis, confocal laser scanning microscopy (CLSM) and scanning electron microscopy (SEM)).

In the **Chapter 3** is described a study of the sodium hydroxide diffusion in chitosan hydrogels, using hydrogel samples having disk geometry (linear diffusion) and cylindrical geometry (radial diffusion). In this aim there were performed experiments of NaOH release from chitosan hydrogels impregnated with NaOH aqueous solutions. This was accomplished by immersing the hydrogel samples in distilled water under mixing and measuring the time evolution of NaOH concentration in the resulted water solution (by the pH-metric method). A mathematical model, obtained from NaOH balance equations inside the hydrogel sample and external aqueous solution respectively, permitted to calculate the time evolutions of NaOH concentration in the system. In the description of the NaOH transport inside the gel, it was used the Fick's law. A mass transfer coefficient was assumed to describe the resistance opposed to the coagulant transfer from the hydrogel sample to the external liquid. The values of the diffusion coefficient in hydrogel and of the external mass transfer coefficient were estimated by the least square method combined with repetitive process simulations. The accuracy of the results obtained by this method was not fully satisfactory, mainly due to different factors (inherent errors in the pH measurements, the possible changes in the gel structure during the interval between their preparation and their use in experiments, the errors in the measurement of disk thickness, the changes in the NaOH concentration in the solution due to the absorption of carbon dioxide from air etc.). However, these results represented a good starting point for the diffusion coefficient determination in coagulation studies, described in the next chapters.

In the **Chapter 4** is presented the study of the chitosan coagulation and the determination of coagulant diffusion coefficient, from better controlled linear diffusion experiments. In this aim it was used a special diffusion cell and a microscope connected on-line to a computer. The time evolutions of the hydrogel thickness, measured by the microscope and stored with a selected frequency, permitted to calculate more accurately the NaOH diffusion coefficient. The calculations were based on a process mathematical model similar with the one described in the previous chapter. The process simulations revealed interesting results regarding the time and space evolutions of NaOH concentration as well as their dependencies on the chitosan and NaOH concentration.

Chapter 5 presents the study of the chitosan coagulation in cylindrical geometry (involving essentially radial diffusion of NaOH), with application in the manufacture of the chitosan fibers. In the first part of the study, there were determined the diffusion coefficients of the sodium hydroxide

through chitosan hydrogel samples having cylindrical geometry. A comparison between diffusion coefficient values observed in linear and radial diffusion evidenced that the measured values from radial diffusion are smaller. This observation is in accord with other published results and is attributed to both process geometry and hydrogel physical structure. The second part of this study approached the wet-spinning process modelling and is based on experiments performed in a small scale plant existing in the Laboratory of Polymer Materials Engineering of the University Claude-Bernard Lyon. The diffusion coefficient measured in the first part of the study was used in the spinning process simulation, based on the developed mathematical model. The good concordance between the calculated and experimental fiber thickness values confirmed the adequacy of the approach.

The thesis ends with a section presenting the general conclusions.

CHAPTER 1. LITERATURE REVIEW

1.1 Chitosan

1.1.1 Definition, sources and structure

The chitosan is a polysaccharide derived from chitin. After the cellulose, the chitin is considered the second most abundant polysaccharide in the world. The chitin can be found in the exoskeletons of arthropods (e.g. insects, crevettes, crabs etc.) in the endoskeletons of cephalopods (e.g. squid, cuttlefish etc.), in the cell walls and the extracellular matrix of certain fungi, yeasts and algae (Muzzarelli and Muzzarelli., 2005)

The chitin and chitosan are polysaccharides composed of 2-acetamido-2-deoxy-β-D-glucopyranose (GlcNAc) and 2-amino-2-deoxy-β-D-glucopyranose (GlcN) units linked by a β-(1→4) glycoside bond (figures 1.2). The chitosan molecule can be considered as derived of cellulose molecule by replacing a hydroxyl group with an amino group at position C-2 (Pillai et al., 2009).

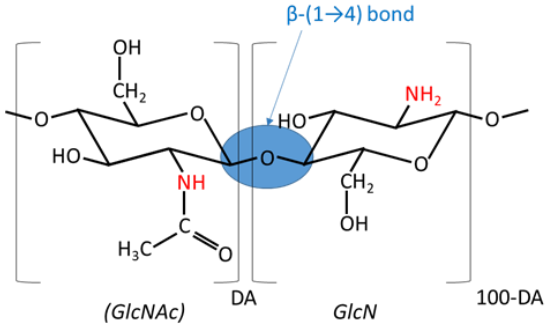

Figure 1.2. Chemical structure of chitin and chitosan; GlcNAc represent glucopyranose acetamido unit and GlcN is glucopyranose amino unit; DA is the degree of acetylation.

In contrast to chitin, chitosan is rarely found in nature. However, it is possible to find it in small quantities in dimorphic fungi such as Mucor rouxii where it is formed by the action of the enzyme deacetylase on chitin (Hudson and Jenkins, 2002). However, the main source for the market of chitosan is the chemical modification of chitin. The chitin and the chitosan have the same generic structure but are differentiated by the mole fraction of acetyl residues in the copolymer. This parameter is called degree of acetylation (DA) and is defined by the relation (1.1).

$$DA = \frac{n_{GlcNAc}}{n_{GlcNAc} + n_{GlcN}} \times 100 \qquad \textbf{(1.1)}$$

n_{GlcNAc} - mole fraction of glucopyranose acetamido unit; n_{GlcN} - mole fraction of glucopyranose amino unit.

A difference between chitin and chitosan consists in the possibility of solubilizing in diluted acid medium, where the chitin is insoluble, while the chitosan is soluble. The border between chitin and chitosan can be traced around a degree of acetylation level of 60% (Domard and Domard, 2001a) (Figure 1.2). Other authors consider this border situated at a DA of 50%. A polymer with a DA less than 50% is called chitosan and a polymer with DA greater than 50% is called chitin (Khor, 2001). Usually, the term chitosan denotes a group of polymers derived from chitin, obtained by deacetylation, rather than a well-defined compound (Aiba, 1991).

1.1.4 Chitosan behavior in solution

1.1.4.1 Solubilization

The solubilization of chitosan is influenced by its structural parameters (DA, Mw) and by the environment parameters such as the pH, the ionic force and the dielectric constant (Domard and Domard, 2002). Because of its acid-base properties, chitosan is considered soluble in aqueous solutions having pH between 1 and 6. This pH range widens as DA increases.

1.1.5 Biological properties of chitosan

The chitosan presents interesting biological properties such as biocompatibility, biodegradability, non-toxicity, hemostasis, healing, antibacterial, and bacteriological and fungistatic properties. All those properties make the chitosan an important supplier for materials used in biomedical applications in vivo and in vitro.

1.1.6 Chitosan applications

The chitosan and its derivatives are used today, or envisaged to be used, in many fields of applications: agriculture (Hadwiger, 2013), packaging (Van Den Broek et al., 2015), adhesives (Patel, 2015), textile industry (Mohammad, 2013), cosmetic products (Jimtaisong and Saewan, 2014), separation technologies (Wan Ngah et al., 2011) and biomedical (Dash et al., 2011; Jayakumar et al., 2010). In the biomedical field, chitosan can be used for tissue engineering (Muzzarelli, 2009; Croisier and Jerome, 2013; Patrulea et al., 2015), vectorization of the active principles (Bhattarai et al., 2010; Casettari and Illum, 2014; Bernkop-Schnürch and Dünnhaupt, 2012) or for other technologies such as bioimaging (Agrawal et al., 2010) or biosensors (Suginta et al., 2012).

The list of biomaterials developed from physical chitosan hydrogels for tissue engineering applications is quite broad, several systems proving a real potential, with particular bioactive properties.

1.2 Chitosan Hydrogels

1.2.1 Definition of a hydrogel

The definition of a gel is given by Aleman et al. (2007): “A gel is a polymer network or a non-fluid colloidal network that is expanded throughout its whole volume by a fluid. A hydrogel is a gel in which the swelling agent is water”.

These general definitions of the "hydrogel" term make it possible to include in this category many materials with very different structures, physicochemical and biological properties. A hydrogel can be defined more precisely depending on several parameters.

1.2.2 Classification of hydrogels

The hydrogels can be classified depending on the preparation methods (homopolymers, copolymers and interpenetrating polymers), ionic charges (nonionic hydrogels, cationic hydrogels, anionic hydrogels, ampholytic hydrogels), source (natural hydrogels, hybrid hydrogels, synthetic hydrogels), physical properties (smart hydrogels, conventional hydrogels), biodegradability (biodegradable hydrogels, non-biodegradable hydrogels), crosslinking (physical crosslinked hydrogels, chemical crosslinked hydrogels).

The chitosan hydrogels are nonionic, natural and conventional ones, which can be of two types, following the preparation method: chemical hydrogels (crosslinked) and physical hydrogels.

1.2.3 Chemical and physical hydrogels of chitosan

In the chemical hydrogels, the macromolecules are interlinked by covalent bonds. The crosslinking agents most studied and used for crosslinking between chitosan chains are: glutaraldehyde, glyoxal, diethyl squarate, oxalic acid and genipin (Berger et al., 2004a).

The physical hydrogels are created by weak and partially reversible bonds. The microstructure of the hydrogel can be stabilized by several types of reversible interactions that are localized on "junction zones", possibly multifunctional, which can extend over a distance between 0.1 and 1μm (Ross-Murphy, 1991).

The chemical way for the hydrogels elaboration as a biomaterial is not a recommended option, because it implies a structure denaturation of the chitosan and the crosslinked agent are often toxic. Due this reason, the only way to obtain hydrogels in order to be used as a biomaterial is the physical hydrogels from a chitosan solution without crosslinked agent.

1.3 Chitosan fibers

1.3.2 Production of chitosan fibers

1.3.2.1 Wet spinning of chitosan

The chitosan wet spinning process implies several stages. The first is the solubilization of the chitosan (the obtained solution is also called “collodion”) followed by passing of the collodion through a spinneret immersed in the coagulation bath. The spinning collodion starts to gelate in contact with the coagulation agent, during its passage through the coagulation bath. The next step is the washing (removing the coagulation agent) of the filament followed by the drying of the filament in order to eliminate the contained liquid. Finally, the fiber is winding on a reel.

A scheme of the chitosan wet spinning process is presented in Figure 1.14.

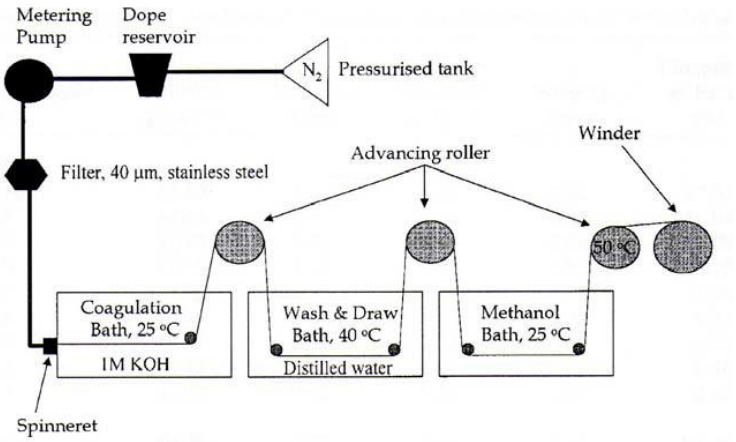

Figure 1.14. A scheme of the chitosan wet spinning process (Knaul, 1998).

1.4 Diffusion in polymer solutions and hydrogels

1.4.1 Introduction

The diffusion is the movement process of a substance from a region (rich in this substance) to another part of the system (poor in the substance) (Crank, 1975). The movement is due the random molecular motions. The diffusion depends on temperature, pressure, viscosity and solute size. The diffusion is fast in gasous phase, slower (several hundreds times) in liquid phase and much slower in solid phase (Cussler, 1997). In polymers and hydrogels, the diffusion process is complex and its rate is placed between the rates in liquid and solid.

In the study of the diffusion processes, very often is used the Fick's first law, quantitatively described by the Equation (1.3).

$$j = -D \cdot \frac{\partial C}{\partial z} \qquad \textbf{(1.3)}$$

1.4.2 Diffusion models and theories

There were proposed several theories and physical models to describe the diffusion process in polymer solutions and gels: free volume models, obstruction effects models, hydrodynamic theories, combined obstruction and hydrodynamic effects etc.

1.4.2.2 Models based on the obstruction effects

The models of this class are hypothesizing that the polymer chains in polymer solutions or gels are impenetrable and have static positions in respect with the diffusing molecules. As result it is appearing an increase of the trajectory traveled by the diffusing molecules, forced to bypass the polymer ones (Amsden, 2002).

1.4.2.2.1 The Maxwell–Fricke model

In accord with this model, the diffusion coefficient is calculated by the Equation (1.12):

$$\frac{D_{ef}\left(1-\varphi\right)}{D_0}=\frac{1-\varphi'}{1+\frac{\varphi'}{\chi}} \quad \textbf{(1.12)}$$

D_{ef} - effective diffusion coefficient; D_0 - diffusion coefficient in solvent without polymer; φ - polymer volume fraction; φ' - volume fraction of the polymer plus non-diffusing solvent bound to the polymer; χ – shape factor of solvent (1.5 for rods and 2.0 for spheres).

The Maxwell–Fricke model is recommended for the diffusion systems involving small molecules in polymer solutions having small polymer concentrations.

1.4.2.2.2 The model of Mackie and Meares

The authors of this model used the theory formulated by Fricke for the electrolytes diffusion in resin membranes. They hypothesized that the polymer mobility is negligible in respect with those of ions and water. As mentioned above, during the diffusion in a polymer solution, the presence of polymer macromolecules, acting as obstacles, are inducing an increase of the distance travelled by the diffusing particles. According to this model, the effective diffusion coefficient of a relatively small particle, can be evaluated by the Equation (1.13):

$$\frac{D_{ef}}{D_0}=\left[\frac{1-\varphi}{1+\varphi}\right]^2 \quad \textbf{(1.13)}$$

In this expression, the notations have the same significances as in the expression (1.12).

1.4.2.2.3 The model of Wang

A first equation for prediction of diffusion coefficients in gels was proposed by Wang (Lauffer, 1961; Westrin et al., 1994), assuming that the decrease of diffusion coefficient in a gel, as compared to that in the free solution, is proportional to the volume fraction of the polymer in the gel:

$$\frac{D_{ef}}{D_0}=1-\alpha\varphi \quad \textbf{(1.14)}$$

D_{ef}, D_0 and φ have the same significances as in previous relations; α – shape parameter (1.5 for prolate; 3 for oblate ellipsoids; 1.67 for randomly oriented rods (Lauffer, 1961; Massaro and Zhu, 1999).

CHAPTER 2. EXPERIMENTAL METHODS USED IN THE CHITOSAN HYDROGELS PREPARATION AND CHARACTERIZATION

2.3 Preparation of the chitosan solution

In order to obtain a final chitosan solution having a chitosan concentration around *w* % (in weight), *w* g of chitosan was weighed and added to 120 mL water into a vessel provided with mechanical mixing (theoretically, the volume of water should be ~100 mL but in order to compensate the water evaporation during the mixing, it is necessarily to add ~ 20 % volumetric extra water). Finally, a stoichiometric volume of glacial acetic acid was added (659 μL, calculated using the equations (2.2) and (2.3)) in order to protonate the amino sites in accordance with the degree of acetylation. The solution was kept at room temperature under mixing (50 rpm) over the night

(approximately 18 hours). Next, the obtained chitosan solution (collodion) was centrifuged for 10 minutes at 5000 rpm, in order to eliminate the air bubbles. In Table 2.1 are presented the properties of the chitosan used in this study.

$$m_{AcOH} = \frac{m_{chitosan}\left(1-DA\right)\left(1-H_{water}\right)M_{AcOH}}{M_{av}} \quad \textbf{(2.2)}$$

$$V_{AcOH} = \frac{m_{AcOH}}{\rho_{AcOH}} \quad \textbf{(2.3)}$$

$$M_{av} = M_{GlcNAc}DA + M_{GlcN}\left(1-DA\right) \quad \textbf{(2.4)}$$

m_{AcOH} - mass of acetic acid (g); $m_{chitosan}$ – mass of chitosan (in the considered example, 2 g); DA – degree of acetylation of chitosan (as a fraction); H_{water} – water concentration in chitosan (mass fraction); M_{AcOH} – Molar weight of acetic acid (60.06 g / mol); M_{av} – an averaged molar weight of the two units in the chitosan macromolecule (2-acetamido-2-deoxy-d-glucopyranose and 2-amino-2-deoxy-d-glucopyranose) (g / mol); M_{GlcNAc} – Molar weight of the 2-acetamido-2-deoxy-d-glucopyranose**;** M_{GlcN} – Molar weight of the 2-amino-2-deoxy-d-glucopyranose.

2.5 Physical chitosan hydrogels preparation

2.5.1 Chitosan coagulation

The most used solubilization agent is the acetic acid. In oreder to prepare a chitosan solution, the acid is added in stoichiometric amount in order to protonate all the amino groups of the chitosan molecules. The most used base for chitosan coagulating is sodium hydroxide. The chemical mechanism of chitosan solubilization and coagulation can be resumed as in Figure 2.8.

$$Ch-NH_2 \xrightarrow[H_2O+CH_3COOH]{solubilisation} Ch-NH_3^{\oplus}CH_3COO^{\ominus} \xrightarrow[NaOH]{coagulation} Ch-NH_2 + CH_3COO^{\ominus}Na^{\oplus}$$

Figure 2.8. The mechanism of chitosan coagulation (Ch a chitosan molecule).

The overall mechanism of chitosan coagulation is complex and not fully proven. It results from the diffusion of the base, the neutralization of chains and their association forming the gel. This involves many parameters such as polymer concentration, degree of acetylation, average molar weight, the nature of coagulation agent, concentration of coagulation agent, temperature of the coagulation bath.

2.5.2 Chitosan hydrogel with disk geometry

The chitosan hydrogels in disk form are obtained by using Petri dishes with 30 mm diameter. The Petri dishes were filled with the chitosan solution prepared as described above. The Petri dishes were immersed into a Berzelius glass containing sodium hydroxide aqueous solution and left a set time so that a chitosan hydrogel is obtained. After the desired coagulating time, the Petri dish was removed from the sodium hydroxide solution. The uncoagulated chitosan solution was removed and the hydrogel was placed into a Berzelius glass with deionized water in order to wash out the sodium hydroxide. The washing was carried out until the pH of the hydrogel supernatant was neutral. The process is also shown in Figure 2.10.

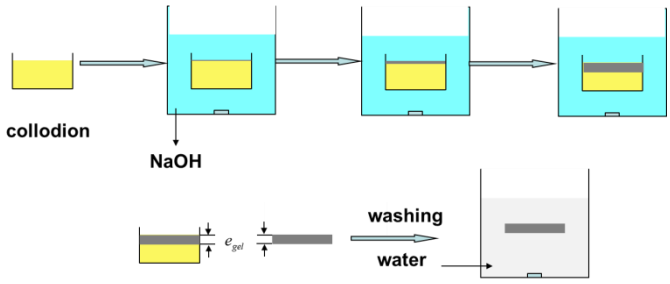

Figure 2.10. Scheme of hydrogel chitosan formation in disk form after partial neutralization of chitosan solutions.

2.5.3 Chitosan hydrogel with cylindrical geometry

An amount of chitosan acidic solution was introduced into a syringe pump connected to a compressed air device. The device has the possibility to modify the flow rate of the chitosan solution by tuning the pressure of the output air. The syringe pump was immersed into a Berzelius glass containing sodium hydroxide aqueous solution. Further, the chitosan solution was injected through the spinneret into the liquid coagulation bath. When attained the desired length of the sample, the pumping was stopped and the coagulation continued. After a given coagulation time, sufficiently long to insure the complete coagulation (approximately 10 minutes), the cylindrical chitosan gel so obtained was extracted from the solution and cut with the aid of scissors. In order to homogenize the concentration of sodium hydroxide into the vessel, a magnetic stirrer, set up at 400 rpm, was used. Finally, the hydrogel cylinder was removed from the coagulating bath and washed to neutral pH, with deionized water. The scheme of the coagulation process is shown in Figure 2.11.

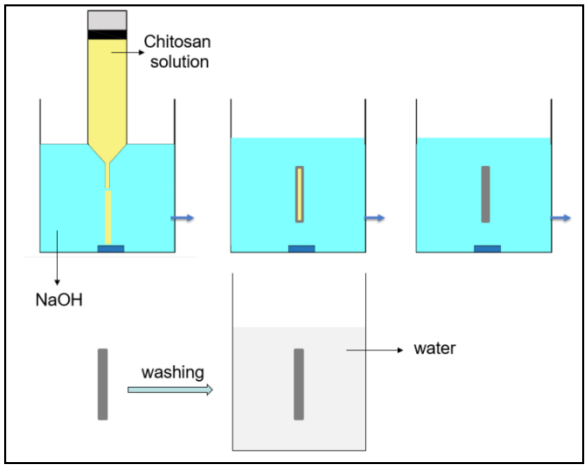

Figure 2.11. Scheme showing the hydrogel chitosan preparation in cylindrical form.

2.6 Characterization of the mechanical properties of the chitosan hydrogels

The measurements were carried using disk shape chitosan hydrogel samples. All the samples had the same thickness (500 μm) and diameter (25 mm). A uniform thickness was insured by using the same chitosan solution amount placed in a Petri dish. The residence time was enough to coagulate all the chitosan solution. In order to have hydrogels with the same diameter, a cutting punch with 25 mm in diameter was used.

The measurements were performed at 20 ° C, by using a rheometer AR2000Ex (TA Instruments) with plane-plane geometry. To avoid the water evaporation from the hydrogel during the experiment, an anti-evaporation system and a solvent trap plate (superior) filled with deionized water were used.

In Figure 2.15 is illustrated the influence of the NaOH concentration in the solution used in coagulation process, on the elastic modulus, *Ge*, of chitosan hydrogel, at equilibrium. As observed from this diagram, the modulus *Ge* increases with the increase of the NaOH concentration, over all the domain of chitosan concentrations. Consequently, it is expected that two chitosan hydrogels containing the same polymer mass fraction but obtained by using different concentrations of sodium hydroxide, to have different values of the diffusion coefficient of sodium hydroxide. For example, the diffusion coefficient for a hydrogel coagulated with a solution 7M NaOH should have a lower diffusion coefficient than a chitosan hydrogel coagulated with a solution 1 M NaOH

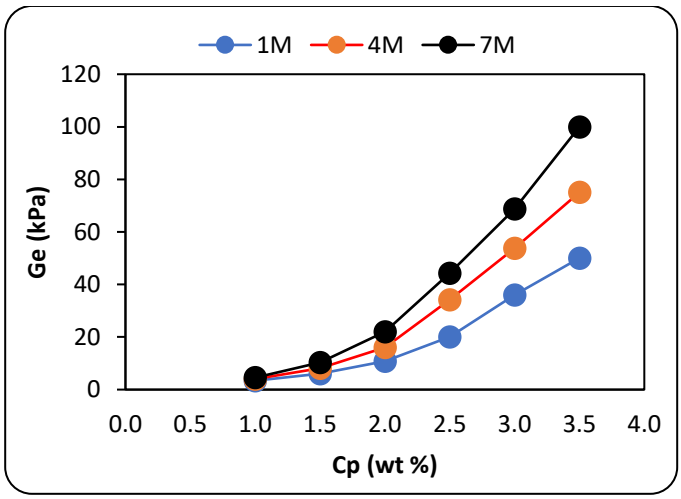

Figure 2.15. Influence of the chitosan concentration (wt %) on the hydrogel elastic modulus.

2.7 Study of the hydrogels microstructures by confocal laser scanning microscopy (CLSM)

The hydrogel's microstructures were investigated by using confocal laser scanning microscopy (CLSM) in reflected light or fluorescence, which is an alternative and complementary method of the cryo-scanning electronic microscopy (cryo-SEM) (Vermonden et al., 2012). By using this technique, the structure of a chitosan hydrogel can be observed directly.

2.7.1 Effect of the chitosan concentration on the hydrogel microstructure

To investigate the influence of the chitosan concentration on the hydrogel microstructure, six chitosan concentrations between 1 % and 3.5 % were considered. The results are presented in Figure 2.19. For the considered hydrogel thickness (350 μm) the microstructures were observed for the 1%, 1.5 % and 2% chitosan concentrations and were not observed for the other chitosan concentrations. In order to observe the microstructure for the hydrogels prepared with higher polymer concentrations, it is necessary to use hydrogels with high thickness. In this case it was observed that the number of the capillaries in such microstructures decreases with the increase of the polymer concentration.

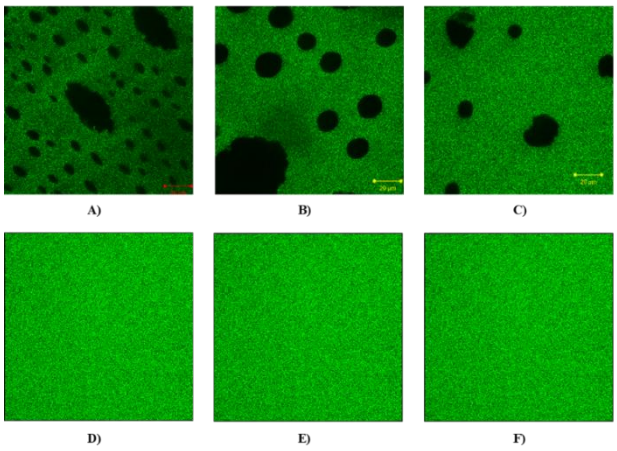

Figure 2.19. CLSM micrographs of physical chitosan hydrogels measured 350 μm from the gel's top and prepared from aqueous chitosan solutions with polymer concentrations (A) 1.0 % (w/w), (B) 1.5 % (w/w), (C) 2 % (w/w), (D) at 2.5 % (w/w), (E) 3 % (w/w), (F) 2 % (w/w) and neutralized using 1 M sodium hydroxide solution.

CHAPTER 3. STUDY OF NAOH DIFFUSION IN HYDROGELS BY NAOH RELEASE FROM HYDROGEL SAMPLES

3.1 Methods

The preparation technique of the hydrogel samples having disk and cylindrical form is described in the paragraph 2.5. A fresh hydrogel disk or cylinder, was fully impregnated with a sodium hydroxide solution of known concentration. Then, the impregnated hydrogel sample was immersed in a known volume of distilled water, subsequently recording its pH variation in time. The measured pH value permits to directly calculate the hydroxyl (HO^-) concentration knowing the ionic product of water at the working temperature.

3.2 Mathematical modeling of the process of NaOH release from chitosan hydrogel. The procedure used for the calculation of NaOH diffusion coefficient in chitosan hydrogel.

3.2.1 Mathematical model of the NaOH release from disk shaped hydrogel

The following assumptions were used in order to characterize quantitatively the sodium hydroxide diffusion process, during an experiment: (1) as the thickness of the disk gel is much smaller than the disk gel diameter, the NaOH transport is considered only through the two circular surfaces, neglecting the transport through marginal (edge) surfaces; (2) the process of sodium hydroxide transport inside the hydrogel disk is symmetrical. Therefore, only a half of hydrogel disk thickness was considered; (3) the flux is null in the center of disk; (4) an equilibrium state is instantaneously established at the hydrogel-liquid interface, between the concentrations of sodium hydroxide in the external liquid and chitosan gel respectively; (5) the mass transfer between the gel and the external liquid is described by the film theory. A mass transfer coefficient, k_L, is considered to define the intensity of mass transfer between the gel and the liquid solution; (6) initially, the NaOH concentration is the same in all points of disk, equal to the concentration of impregnating solution; (7) the liquid solution outside the hydrogel is perfectly mixed.

The coexistence of two phases (hydrogel and liquid), implies the necessity to write the NaOH balance for the both phases.

3.2.1.1 The NaOH balance in the gel phase of the system

Since the only phenomenon occurring inside the gel is an unsteady state sodium hydroxide transport by diffusion, the space and time variations of NaOH concentration is described by the second law of Fick:

$$\left(1-\varepsilon\right)\frac{\partial C}{\partial t} = D_{ef}\,\frac{\partial^2 C}{\partial x^2} \qquad \textbf{(3.2)}$$

where *C* is the liquid NaOH concentration inside the gel, ε is the polymer fraction inside the gel and *Def* is the NaOH effective diffusion coefficient.

The boundary conditions associated to the differential equation (3.2) are established in two points, the solution interface (x = L) and the center of the disk (x = 0).

On the gel interface is assumed an equilibrium between the NaOH concentrations in the two phases ($C_i(t)$ in liquid and C(L,t) in the gel), characterized by the relation definig the partition coefficient (K) :

$$K = \frac{C\left(L,t\right)}{C_i\left(t\right)} \qquad \textbf{(3.3)}$$

On the gel-solution interface (x=L), the mass flux continuity is assumed, expressed by the equation:

- **t >0, x=L**, $k_L\left(C_i - C_{liq}\right) = -D_{ef}\,\frac{\partial C}{\partial x}$ **(3.4)**

where k_L is the mass transfer coefficient in the liquid film adjacent to gel interface.

The flux in the disk center is null:

- **t > 0, x = 0,** $\frac{\partial C}{\partial x} = 0$ **(3.5)**

Initially (at the beginning of experiment), the sodium hydroxide concentration across the gel is constant:

- **t = 0, 0 ≤ x ≤ L**, $C\left(x,0\right) = C_{gel,0}$ **(3.6)**

The equation (3.2) was solved numerically by the method of lines (Kiusalaas, 2005).

3.2.1.2 The NaOH balance in liquid phase of the system

In the hypothesis that the liquid phase is perfectly mixed, the NaOH balance is given by equation:

$$V_{liq}\frac{\partial C_{liq}}{\partial t}=S\left(-D_{ef}\frac{\partial C}{\partial x}\right)_{x=L}=Sk_L\left(\frac{C_N}{K}-C_{liq}\right) \qquad \textbf{(3.22)}$$

Where V_{liq} represents the deionized water volume used in experiment and S represents the disk surface area in contact with the liquid phase.

3.2.1.3 Results and discussion

The mathematical model described above permits to calculate the time evolution of NaOH concentration in the solution, as resulting from its release from the gel disk. In this aim, the differential equations (3.19) and (3.22) were integrated numerically using MATLAB software (the function "ode45" for the integration of differential equations). However, the integration results are depending on the parameters D, K and k_L.

Due to the particularity of the experimental system (floating gel disk inside a stainless-steel tea strainer, limited liquid mixing in the neighborhood of the gel) the mass transfer coefficient between the gel disk and the outside liquid, cannot be evaluated with a reasonable reliability from the published correlations. However, the published correlations could indicate, at least as the order of magnitude, its value. In the case we are investigating, the mass transfer phenomenon is in some similarity with that occurring between a rotating disk (with fixed spatial position) and a liquid. For this system it was proposed the correlation (Cussler, 2007, Table 8.3-3):

$$\frac{k_L d}{D}=0.62\,\mathrm{Re}^{1/2}\,Sc^{1/3};\ \mathrm{Re}=\frac{\rho\omega d^2}{\eta};\ Sc=\frac{\eta}{\rho D} \qquad \textbf{(3.22)}$$

d- dimeter of the disk; D- NaOH diffusion coefficient in solution; ω – rotation speed of the disk; ρ, η- density and dynamic viscosity of the solution.

Considering the physical properties of the liquid water: $\rho=1000$ kg/m^3; $\eta=10^{-3}$ kg/(ms), $D=1.75\cdot10^{-9}$ m^2/s (Farry, 1966) and $\omega=0.3$ rot/s, one obtains: $k_L=2.2\cdot10^{-5}$ m/s.

Another approximation of the diffusion coefficient can be obtained by its definition in accord with the film theory:

$$k_L=\frac{D}{\delta_L}\text{, } (\delta_L\text{- liquid film thickness}) \qquad \textbf{(3.23)}$$

Considering a typical value for the liquid film thickness, $\delta_L=0.1$ mm$=10^{-4}$ m (Cussler, 2007), one obtains: $k_L=1.75\cdot10^{-5}$ m/s.

The values of the effective NaOH diffusion coefficient in the gel, D_{ef}, could be evaluated using the relations presented in Chapter 1. The difficulty in the use of these relations comes from the unsteady-state character of the process (variation of NaOH concentration in the system) and the lack of data regarding the dependence of NaOH diffusion coefficient on the solution concentration. Nevertheless, for the diffusion coefficient value given above, by using the relations (1.12). (1.13) and (1.14), there were obtained the values presented in Table 3.1. Using these values of D, combined with the approximated values for k_L, in the simulation of the experiments described above, the agreement between the calculated and experimental results was inadequate.

As no reliable data are available for the calculation of the parameters D and k_L, their values were estimated from the measured time evolutions of pH in the solutions outside the gel samples, as explained in previous paragraphs. The estimation calculations were performed by the least square method, using the "lsqcurvefit" function of MATLAB.

Considering the overall accuracy of the measurements and its averaging character, we neglected the variation of mass transfer coefficient with the concentration of the impregnating solution, using the same value of k_L in all the estimations. The best estimated value obtained in this way, was $k_L=1.85\cdot10^{-5}$ m/s, which is in a rather good agreement with the theoretical evaluations presented above. So, finally the values of the D_{ef} were estimated using this value.

The experiments were repeated with gels having different chitosan concentrations, gels obtained by coagulation with different coagulant concentrations and gels impregnated with NaOH solutions having different concentrations. In figures 3.7 and 3.9 are presented the diffusion coefficient values estimated from data obtained by keeping constant each one of these parameters.

The data presented in figures 3.7 and 3.9 are evidencing a decrease of the NaOH effective diffusion coefficient in the gel with the increase of the NaOH concentration in the solution used as coagulant for gel preparation. This is assumed to occur due to the denser structure of the gel, formed at higher coagulant concentrations (see chapter 2). In the same time, the diffusion coefficient is increasing with the decrease of the NaOH concentration in the impregnating solution. Presumably, this is the effect of the increase of NaOH diffusivity in aqueous solutions with the decrease of NaOH concentration (Farry, 1966). However, the results presented in the first two figures do not evidence a clear dependence of the effective diffusion coefficient in respect with the chitosan concentration in the gel.

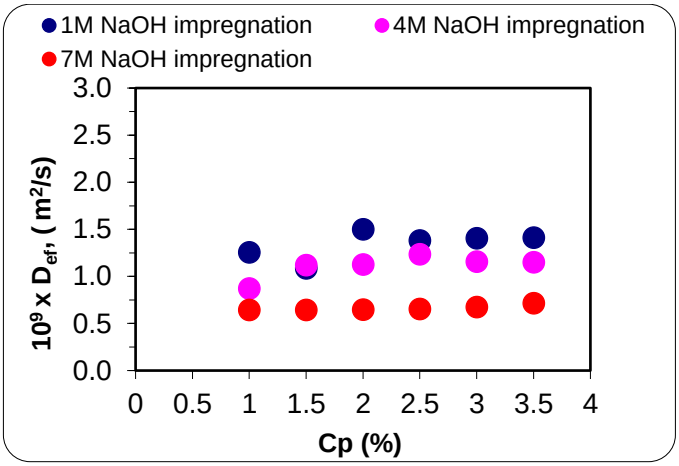

Figure 3.7. The calculated values of NaOH diffusion coefficient in hydrogels of disk shape, with different chitosan concentrations and different concentrations of the impregnating NaOH solution (all hydrogels were prepared with NaOH 7M as coagulant).

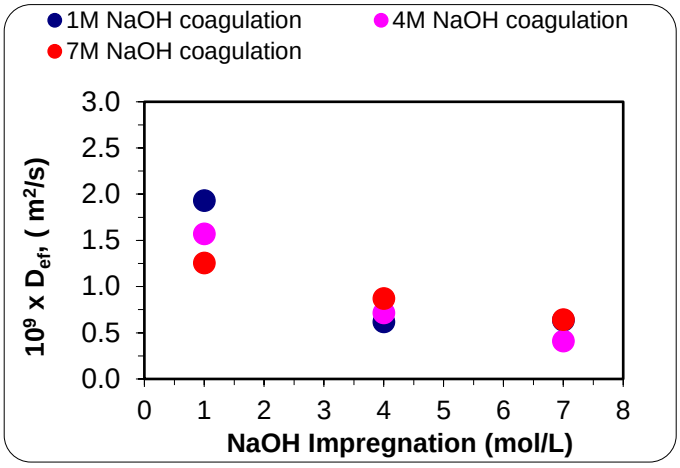

Figure 3.9. The calculated values of NaOH diffusion coefficient in hydrogels of disk shape, prepared with different coagulating concentrations of NaOH, versus NaOH concentration in the impregnating solution (chitosan concentration 1 wt % for all hydrogels)

This suspicious results could be explained by multiple factors: the experimental error in the measurement of the pH, the unsteady character of the process, the limited mixing of the liquid, the non-homogeneities occurring in the gel structure appearing during the coagulation process (see chapter 2), the possible changes in the gel structure during the interval between their preparation and their use in experiments, the errors in the measurement of disk thickness, the changes in the NaOH concentration in the solution due to the absorption of carbon dioxide from air etc.

3.2.2 Mathematical model of the NaOH release from hydrogels having infinite cylinder geometry (radial diffusion*)*

The principle of determination of NaOH diffusion coefficient in hydrogels having cylindrical shape is the same as in the hydrogel disk, the equation of diffusion (the second law of Fick) being written for cylindrical geometry. So, both the experimental and theoretical (modelling) treatment is very similar to the one described in the preceding paragraph.

3.2.2.3 Results and discussion

In Figures 3.14 and 3.16 are presented the values of the effective diffusion coefficient determined at different concentrations of the impregnating solution, chitosan concentrations in the gel and NaOH concentrations used for the gel preparation.

The values are delimited in the interval 10^{-9} to 1.310^{-9} m^2/s. From the figures 3.14 and 3.16 is observed a slight decreasing trend of the diffusion coefficient with the increase of chitosan concentration, not observed in the case of disk geometry. The dependences in respect with the NaOH concentrations in the coagulating solution and impregnating solution respectively are less evident but seem to be present.

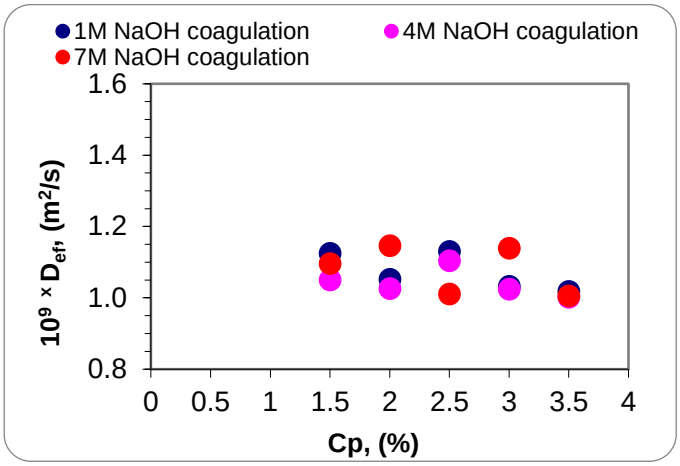

Figure 3.14. The diffusion coefficient values for the sodium hydroxide through the chitosan hydrogels having infinite cylinder geometry at different chitosan concentrations (Cp) impregnated with NaOH 7M. The legend indicates the coagulating NaOH concentrations.

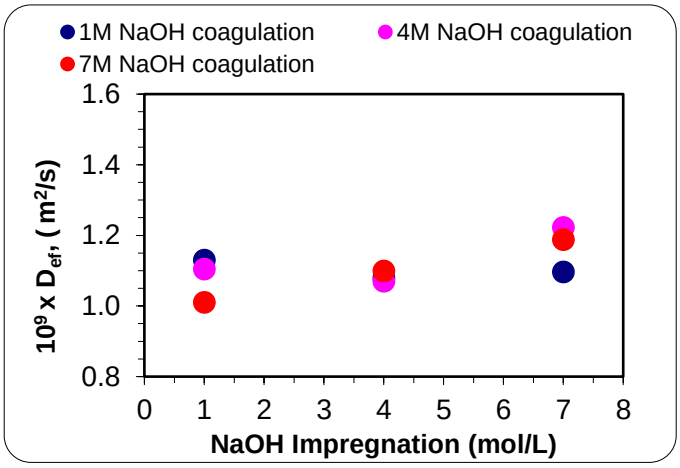

Figure 3.16. The diffusion coefficient values for the sodium hydroxide through the chitosan hydrogels having infinite cylinder geometry versus the concentration of impregnating solution; chitosan concentration 2.5 wt%. The legend indicates the NaOH concentration used in the coagulation.

A comparison between the results obtained in the two set of experiments is presented in the parity diagram, given in Fig. 3.18. The points in the diagram represent pairs of diffusion coefficient values, obtained in identical working conditions, in the two types of experiments. As observed from this figure, the dispersion of the results for the experiments conducted in the disk geometry is very important, much higher than those obtained from cylindrical geometry. So, the values determined from the experiments with cylindrical samples seem to be more reliable. The rather high values of the effective diffusion coefficient measured for the disk geometry in this group, higher than those reported for the diffusion coefficient in solution, make them less reliable. Therefore, we can consider that the most reliable values are in the groups (a) and (b), including the higher number of points. From these two groups it can be inferred an overall averaged value for the NaOH diffusion coefficient in chitosan gels, determined in the working conditions, of $1.2 \cdot 10^{-9}$ m^2/s.

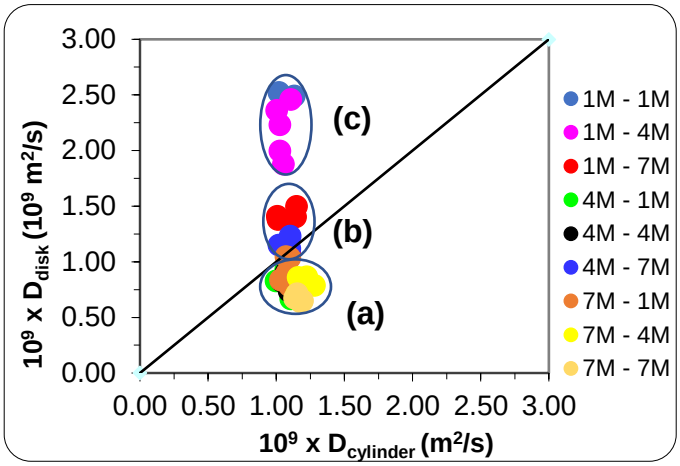

Figure 3.18. Comparison between the averages values of D_{ef} in disk and in cylinder assuming K=1 and k_L=1.85 x 10^{-5} m/s.

CHAPTER 4 STUDY OF THE CHITOSAN COAGULATION KINETICS BY EXPERIMENTS IMPLYING LINEAR DIFFUSION

4.1 Materials and Methods

The coagulation experiments were performed in a transparent quartz cell (volume 350 μL) manufactured by Hellma Analytics (type 100 QS/100-1-40), having the outer dimensions 45x12.5x3.5 mm, light path of 1 mm and inner width 9.5 mm. This was carefully filled with chitosan solution and was immobilized (by a double-sided tape) on the bottom of a Petri dish (100 mm in diameter), filled thereafter with a volume of 80 mL aqueous solution of *NaOH*. The kinetics of coagulation was investigated by measuring the time evolution of the hydrogel volume inside the transparent cell. In this aim, there were registered images of the hydrogel layer, at different coagulation times, by an optical microscope Olympus BX41 (4x objective), coupled with an Olympus DP26 camera, connected on-line to a PC, using Olympus cellSens software (Figure 4.1). All the experiments were conducted at room temperature (25 ^oC).

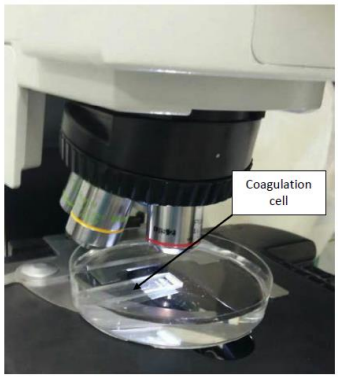

Figure 4.1. Image of the experimental setup for the study of linear coagulation kinetics.

The time evolution of the hydrogel layer thickness, inside the cell, was obtained from the images registered at different coagulation times. In what follows, the interface between the NaOH aqueous solution and the chitosan hydrogel will be named front interface, whereas the interface

between the gel and the chitosan solution will be referred to as coagulation interface (Figure 4.2). Also, the terms hydrogel and gel will be used interchangeably.

4.2 Mathematical model of the coagulation process

In order to build a mathematical model of the coagulation process, we adopted the following hypotheses: (1) the reaction between the $-NH_3^+$ moieties and *NaOH* is much faster than the *NaOH* effective diffusion through the gel, so it will be considered instantaneous (Knaul, 1997); (2) the transport of *NaOH* through the hydrogel occurs only by diffusion, in a single direction, along the cell axis (perpendicular to the hydrogel/dope interface) or in radial direction (in the cylinder geometry experiments); (3) *NaOH* diffusion coefficient is constant across the chitosan hydrogel and in time; (4) *NaOH* concentration in the aqueous solution outside the gel is considered constant during coagulation, due to the large excess of *NaOH*; (5) on the front interface there is fulfilled the condition of NaOH flux continuity; (6) *NaOH* concentration at the hydrogel/dope interface (coagulation interface) is negligible small, with a fast *pH* variation across the coagulation interface (Venault et al., 2012).

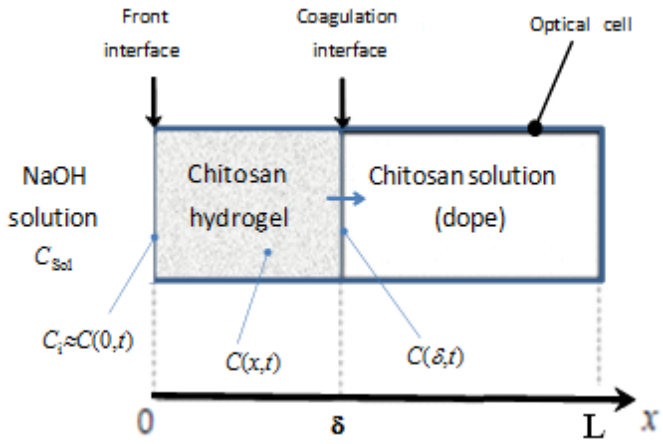

Figure 4.2. Representation of the coagulation system in coagulation/optical cell with notations for the coagulation interface location and concentrations in the different boundaries

According to these hypotheses, the overall process kinetics is controlled by the transport of *NaOH* from the aqueous solution toward the coagulation zone.

The *NaOH* balance equation inside the chitosan hydrogel (second Fick's law) has the general form:

$$(1-\varepsilon)\frac{\partial C}{\partial t} = D_{ef}\frac{\partial^2 C}{\partial x^2} \qquad \textbf{(4.1)}$$

where C is the *NaOH* concentration in the hydrogel. The variable x represents the transport coordinate, having the origin on the front interface.

The initial and boundary conditions associated to Equation (4.1) are (see Figure 4.2):

i) The condition of *NaOH* absence in the dope at the initial time (t=0):

- $\mathbf{t = 0,\ 0 \le x \le L},\ C(x,0) = 0$ **(4.2)**

ii) The *NaOH* flux continuity on the front interface:

- **x = 0, t > 0,** $k_L\left(C_{sol}-C_i\right)=-D_{ef}\dfrac{\partial C}{\partial x}$ **(4.3)**

iii) The condition of null *NaOH* concentration at the coagulation interface (the consumption of *NaOH* is much faster than its transport by diffusion) or null *NaOH* flux, when coagulation is completed:

- **x = δ < L, t > 0,** $C\left(\delta,t\right)=0$ **(4.4a)**

- **x = δ = L, t > 0,** $\dfrac{\partial C}{\partial x}=0$ **(4.4b)**

The time evolution of hydrogel thickness is calculated considering the stoichiometric relation existing between the molar fluxes of *NaOH* and $-NH_3^+$ groups consumed on the coagulation interface *(x=δ)*, defined by the equation:

$$\frac{\partial\delta}{\partial t}=-\frac{D_{ef}}{C_{NH_3^+}}\frac{\partial C\left(\delta,t\right)}{\partial x} \quad \textbf{(4.5b)}$$

The model defined above was solved numerically by the method of lines, presented in Chapter 3.

4.3 Results and discussion

4.3.1 Experimental results

As already described, the chitosan coagulation mechanism involves the reaction of the protonated amino -groups ($-NH_3^+$), of the dissolved chitosan macromolecules, with hydroxyl ions (HO^-) of coagulant, conducting to the neutralization of chitosan chains. Further, the sodium hydroxide is diffusing through the chitosan hydrogel so formed, toward the hydrogel-chitosan dope interface, continuing to neutralize and to increase the hydrogel stratum thickness.

Figure 4.3 presents a snapshot of the hydrogel layer between the two solutions, during the experiment. As can be observed from this figure, the hydrogel and the chitosan dope are separated by a distinct boundary (also observed by Rivas Araiza et al., 2010), indicating a very tinny reaction zone of *NaOH* with solubilized chitosan molecules, consequence of the fast-ionic reaction.

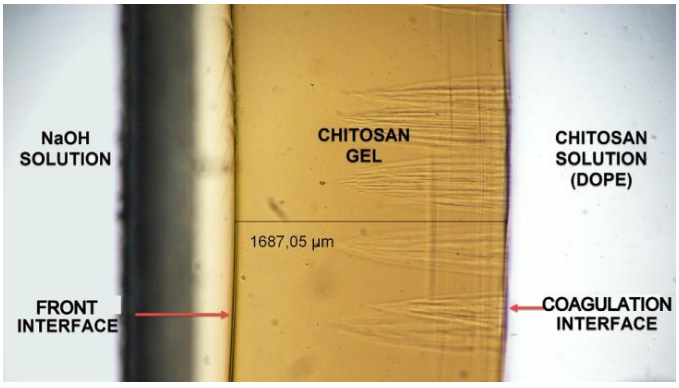

Figure 4.3. A snapshot of the coagulation process.

The coagulant diffusion throughout the two structural zones of the gel is characterized by different resistances and consequently different diffusion intensities. Therefore, the diffusion

coefficient value, inferred from experimental data, is an 'effective' or 'apparent' one, representing an average over the whole structure of the gel. The measured evolutions of hydrogel thickness with coagulation time, for chitosan solutions of different concentrations, are presented in Figure 4.4 and Figure 4.5 for *NaOH* concentrations *1M* and *7M* respectively. As expected, the increase of the gel thickness is faster on the first part of coagulation process, due to the smaller diffusion distance of coagulant between the front interface and the coagulation interface. At longer gelation times, the transport distance inside the gel is larger and the growth rate of the hydrogel is decreasing, becoming almost constant at the end of the coagulation process, where the curves have approximately linear shapes.

As seen from the Figures 4.4 and Figure 4.5, the rate of chitosan coagulation from its aqueous solutions (defined here as the speed of coagulation front) increases with the decrease of chitosan concentration and the increase of coagulation agent concentration.

The decrease of the coagulation front speed with the increase of chitosan concentration is explained by the increased number of $-NH_3^+$ moieties to be neutralized, combined with a slightly higher resistance opposed by solid phase to coagulant diffusion (lower value of NaOH diffusion coefficient in the gel). However, the dependence of coagulation front speed on chitosan concentration is not linear.

At a given coagulation agent concentration and coagulation time, the ratio of the gel thicknesses obtained for two chitosan concentrations is smaller than the reversed chitosan concentrations ratio.

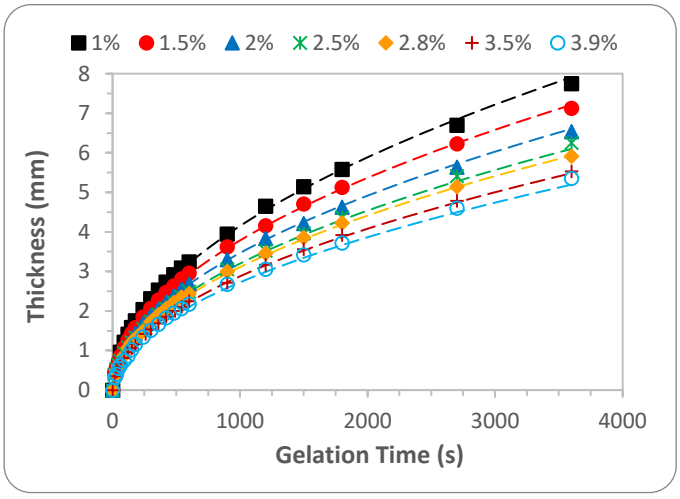

Figure 4.4. Measured and calculated hydrogel thickness versus gelation time, for different chitosan concentrations; symbols- measured values; solid lines- calculated values (NaOH solution 1M). The legend gives the polymer concentration of the solutions (in wt %).

As an example, consider the gels thicknesses calculated for a coagulation time of 2000 s, as resulting from Figure 4.4. The gel thickness is 5.8 mm for the chitosan solution 1 % and 4 mm for the chitosan solution 3.9 %. Even if the NaOH diffusion coefficient values in the two gels are comparable, the gel thicknesses ratio is around 1.45 for a ratio of chitosan concentrations around 4. The explanation resides in the increase of NaOH concentration gradient in the gel with chitosan concentration, i.e. a steeper decrease of NaOH concentration in a more concentrated gel, due to a higher density of neutralized $-NH^{3+}$ groups. This is inducing an acceleration of the diffusion, leading to a higher NaOH

flux on the coagulation interface (Figure 4.6). A similar conclusion can be drawn regarding the influence of coagulant concentration on the gel thickness. As can be observed from Figure 4.4 and Figure 4.5, for a chitosan concentration of 1 %, by increasing the coagulant concentration from 1M to 7M the gel thickness obtained in 3600 s is increasing from 7.8 mm to 9.6 mm. So, a seven-fold increase of NaOH concentration leads to only a 1.24-fold increase of gel thickness.

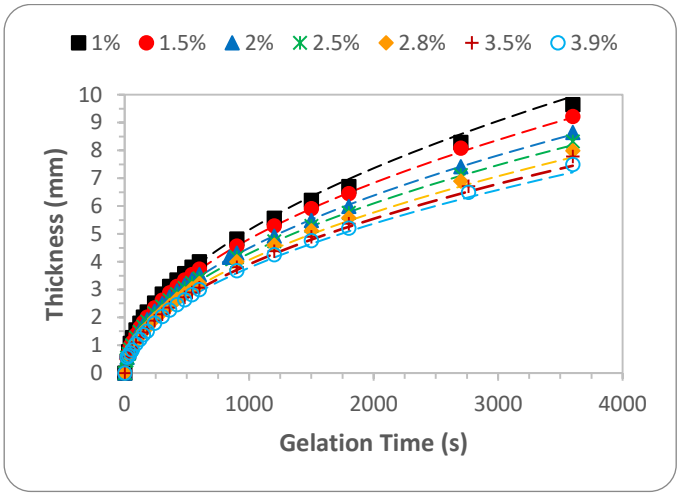

Figure 4.5. Measured and calculated hydrogel thickness versus gelation time, for different chitosan concentrations; symbols- measured values; solid lines- calculated values (NaOH solution 7 M). The legend gives the polymer concentration of the solutions (in wt %).

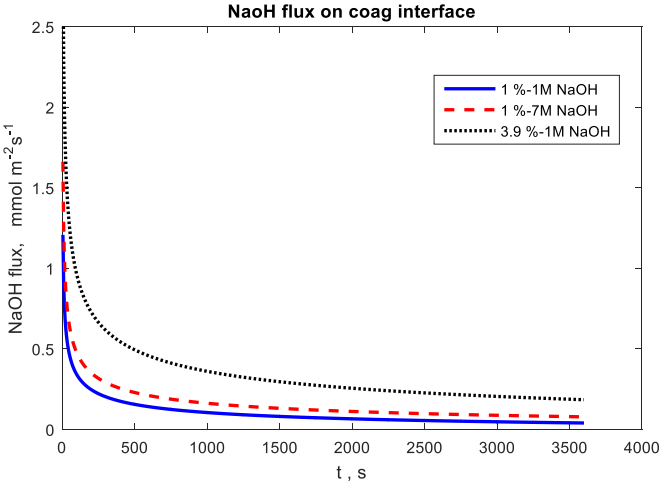

Figure 4.6. Time evolutions of NaOH flux on the coagulation interface (N(δ,t)).

In order to evidence the explanation of this result, we consider the mass balance of *NaOH* during the coagulation time, t_c, defined by the equation:

$$m_f = m_a + m_r \qquad \textbf{(4.10)}$$

$$m_f = S\int_0^{t_c} N(0,t)dt;\quad m_a = S\int_0^{\delta} C(x,t_c)dx;\quad m_r = S\int_0^{t_c} N(\delta,t)dt = S\delta C_{NH_3^+} \qquad \textbf{(4.11)}$$

where m_f, m_a and m_r are the the amounts of NaOH fed into the gel, accumulated into the gel and neutralized respectively.

The NaOH quantity consumed in the coagulation process, m_r, is depending on the NaOH flux at the coagulation front, N(δ,t), which is decreasing in time, due to the increase of resistance opposed to the NaOH transport (Figure 4.6). Similarly, the fed quantity of NaOH into the gel, m_f, is depending on the input flux at the front interface, N(0,t), which is decreasing with time, due to the decrease of concentration gradient on the front interface, as result of NaOH accumulation into the gel (Figure 4.7). The effect of NaOH concentration growth from 1M to 7M, keeping the chitosan concentration constant at 1 %, is a significant increase of mass flux on the front interface and a less important increase of the flux on the coagulation interface (Figure 4.6 and Figure 4.7).

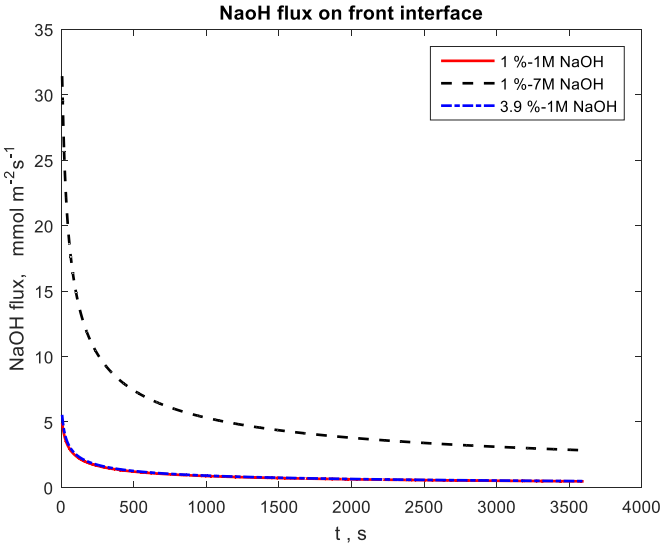

Figure 4.7. Time evolutions of NaOH flux on the front interface (N(0,t)).

The flux on the coagulation interface, when using NaOH solution 7M, is only slightly superior to that corresponding to the solution 1M (Figure 4.6), thus explaining the value of gel thickness, not very different of that obtained with the coagulant concentration 1M.

Nevertheless, the amount of *NaOH* accumulated inside the gel is superior to the amount consumed in the coagulation reaction, the ratio between the two quantities rising with the *NaOH* concentration in the solution used for coagulation.

4.3.2 Simulation of the linear coagulation

The numerical solution of the coagulation process model was calculated by the procedure described previously.

The main parameters of the coagulation process model defined above are the *NaOH* diffusion coefficient inside the chitosan hydrogel, D_{ef}, the liquid-solid (hydrogel) *NaOH* mass transfer coefficient at the front surface, k_L, and the partition coefficient K.

Our preliminary parameter estimations, including K as an unknown parameter, together with *pH* measurements performed in immerged *NaOH* aqueous solutions inside the prepared hydrogels, indicated that the *NaOH* partition coefficient between *NaOH* solution and chitosan hydrogel was close to unity. This is in agreement with the theoretical interpretation of the partition coefficient for non-adsorbed solutes (in the hypothesis of weak interactions between Na^+, HO^- and chitosan), as

representing the geometric exclusion effect, K=1-ε (Muhr et Blanchard, 1982). This corresponds, in our working conditions, to values of K between 0.96 and 0.99.

Similarly, as pointed up by different authors, no general and reliable data are available for the calculation of liquid-solid mass transfer for limiting cases of slow flow or stagnant liquids (Bird et al., 2002).

By applying the least square method, we obtained the value of the mass transfer coefficient, k_L=7.5·10^{-6} m·s^{-1} and the values of D_{ef} presented in Table 4.1, dependent on the chitosan and *NaOH* concentrations. Our calculations indicated that the influence of k_L on the gel thickness is weaker than the influence of D_{ef}; therefore, we used the same value of k_L for both *NaOH* solutions.

The estimated diffusion coefficient values, presented in Table 4.1, are indicating a significant decrease of sodium hydroxide diffusivity in the hydrogel, with the increase of chitosan concentration, most probably due to an increased resistance induced by an increased "solid" volume fraction. In the same time, it can be observed a decrease of the diffusion coefficient with the increase of sodium hydroxide concentration from *1M* to *7M*, possibly due to the increase of solution viscosity and the impact of neutralization conditions on the morphology of the gels and their diffusive resistance.

Table 4.1. Estimated diffusion coefficient values (k_L =7.5·10^{-6} m·s^{-1}).

Chitosan concentration, (wt %)		**1**	**1.4**	**2**	**2.5**	**2.8**	**3.3**	**3.9**
D_{ef} ·10^9, m^2/s	**1M**	1.80	1.75	1.70	1.65	1.55	1.50	1.45
	7M	1.65	1.60	1.55	1.50	1.45	1.40	1.35

In order to check also the reliability of the estimated value of k_L, we appraised it theoretically by several models published in chemical engineering literature. Different authors identified asymptotic values for *Sh* number, characterizing the mass transfer between a solid particle and a surrounding fluid with small or null velocity. A classical value frequently reported for a spherical particle is *Sh* = 2. A limiting value *Sh* = 4 was also found theoretically for regular packing, if based on the local difference between interfacial and bulk concentrations (Bird et al., 2002).

Besides, there are reported values for the *Bi* number characterizing the mass transfer between stagnant liquid zones and solid porous particles in packed beds. Iliuta et al. (1999) found, by tracer experiments, *Bi* values between 1 and 11. In the expression of *Sh* and *Bi* numbers we used the equivalent diameter, $\bar{d}_p$, defined as the diameter of a sphere having the same external surface area (*S*) as the active (open) surface area of the coagulation cell:

$$Sh = \frac{k_L \bar{d}_p}{D}; \quad Bi = \frac{k_L \bar{r}_p}{D_{ef}}$$
$$\bar{d}_p = 2\bar{r}_p \sqrt{\frac{S}{\pi}} \qquad \textbf{(4.14)}$$

Using the cell dimensions of the cell used in our experiments, *Sh* = 2 and *D* = 1.83·10^{-9} m^2/s (an average value), one obtains a mass transfer coefficient value, k_L = 2.1·10^{-6} m·s^{-1}. On the other side, the values of *Bi* between 1 and 11 lead to values of k_L between 1.6·10^{-6} m·s^{-1} and 2.33·10^{-5} m·s^{-1}.

Therefore, we appreciate that the value $k_L = 7.5 \cdot 10^{-6}$ m·s^{-1} is well estimated within the published data ranges.

The comparisons between the calculated and experimental hydrogel thickness values, presented in Figure 4.4, are evidencing a good phenomenological quality of the modeling approach, which, along with the reliability of mass transport parameters values, are demonstrating the suitability of the proposed mathematical model. Typical *NaOH* concentration profiles inside the hydrogel, calculated at different coagulation times are given in Figure 4.11. As can be observed, the *NaOH* concentration at the front interface is not constant, presenting an increasing evolution in time.

This is the result of the increase of gel resistance to the *NaOH* transport toward the coagulation interface, due to the increase of gel thickness. The growing resistance of the gel stratus is inducing a decrease of *NaOH* flux and an increased *NaOH* concentration in the gel volume, *i.e.* a decreasing concentration gradient and an increasing interface concentration (see relation (4.3)).

CHAPTER 5. MATHEMATICAL MODELLING OF CHITOSAN FIBER FORMATION BY WET SPINNING

This chapter presents the studies of the chitosan fiber formation process by wet spinning of the chitosan acid solution. There were performed experimental studies aiming to determine the NaOH diffusion coefficient in cylindrical coagulation (radial diffusion of coagulant) and chitosan wet spinning experiments on a laboratory scale unit. The experimental results were used in a theoretical study aimed to develop a mathematical model useful in the analysis and design calculations of the wet-spinning process. As shown in the previous chapter, the main parameter of the coagulation model is the coagulant diffusion coefficient in the gel. The published studies are evidencing differences between the diffusion coefficient values calculated from linear diffusion experiments, as compared with radial diffusion. Consequently, a first study presented in this chapter regards the determination of the NaOH diffusion coefficient in chitosan gel samples having cylindrical geometry. The diffusion coefficient values so obtained were used in the wet spinning process modelling and simulations study, described in the second part of this chapter.

5.1 Study of the NaOH diffusion in chitosan gels having cylindrical geometry

5.1.1 Experimental study

5.1.1.1 Method

In order to investigate experimentally the coagulating kinetics of chitosan solution (dope) having cylindrical shape (radial diffusion of sodium hydroxide), the chitosan dope samples having cylindrical geometry (filaments) were exposed to coagulating times between 15 s and 5 minutes, keeping constant the working conditions (the same chitosan concentration, temperature and NaOH concentration in the coagulating bath). After a given coagulation time, the chitosan gel tube was removed from the coagulation bath, wiped with filter paper and cut at both ends. Further, the non-coagulated chitosan solution was removed by using compressed air and finally, the tube was sampled in small pieces and passed to microscopy, where the thickness of coagulated chitosan membrane so obtained was measured (Figure 5.1). The microscope used was a Leica M205A stereo.

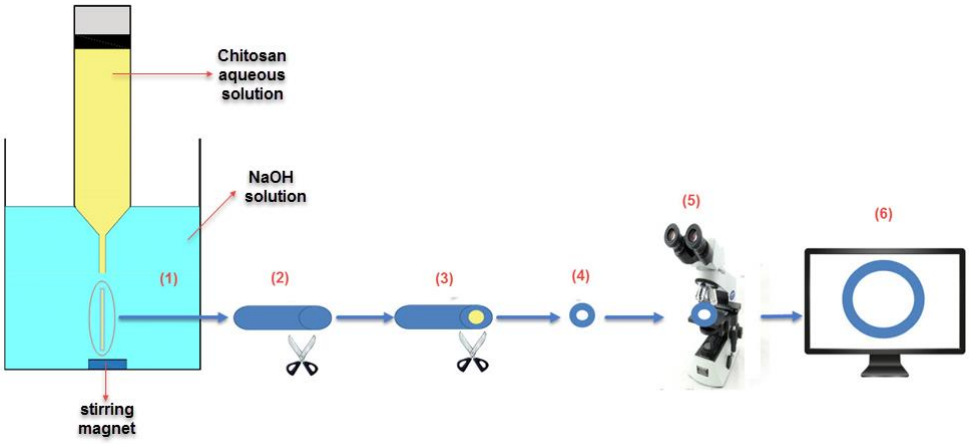

Figure 5.1. The process diagram: (1) coagulated bath; (2, 3) removing the non-coagulated chitosan; (4) cutting the samples; (5) taking the images by using a microscope; (6) measuring the thickness of the coagulated chitosan.

5.1.1.2 Experimental results

In Figure 5.2 is presented a sequence of registered images, illustrating the progress of chitosan hydrogel thickness as a function of coagulation time.

The measured time evolutions of gel thickness, working with chitosan solutions of different concentrations, are presented in Figures 5.3, for sodium hydroxide concentrations 1M, 4M and 7M respectively. As seen from these figures, the rate of chitosan coagulation from its aqueous solutions (the speed of coagulation front displacement) increases with the decrease of chitosan concentration, and the increase of coagulation agent concentration. The explanation of this result stems in the diffusion control of the coagulation kinetics and a higher solid volume fraction of the gels formed from more concentrated chitosan solutions, inducing a stronger hindrance to the sodium hydroxide transport by diffusion.

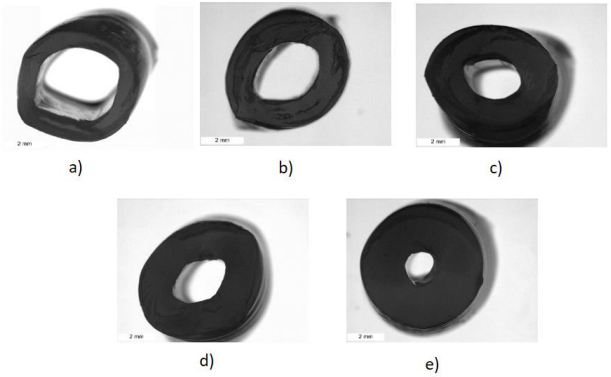

Figure 5.2. The propagation of the gel front for 2% (w/w) chitosan coagulated with 7M NaOH: a) 60 s; b) 120 s; c) 180 s; d) 240 s; e) 300 s.

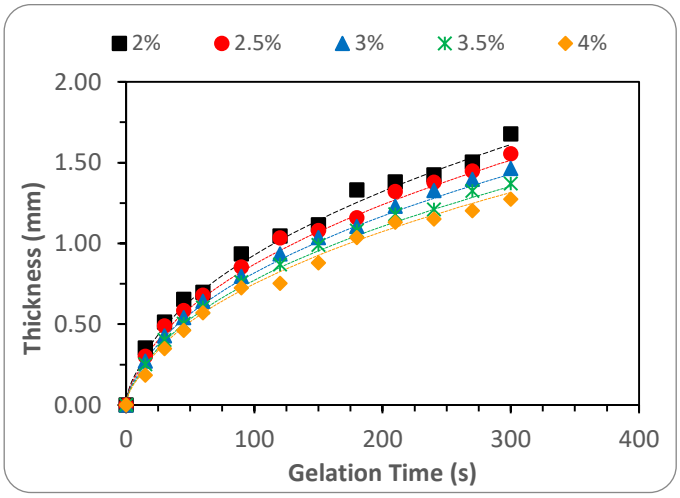

Figure 5.3. Measured and calculated increase of hydrogel thickness as a function of gelation time for different chitosan concentrations; points - measured values; solid lines - calculated values (NaOH solution **1M**). The legend gives the polymer concentration (in wt %).

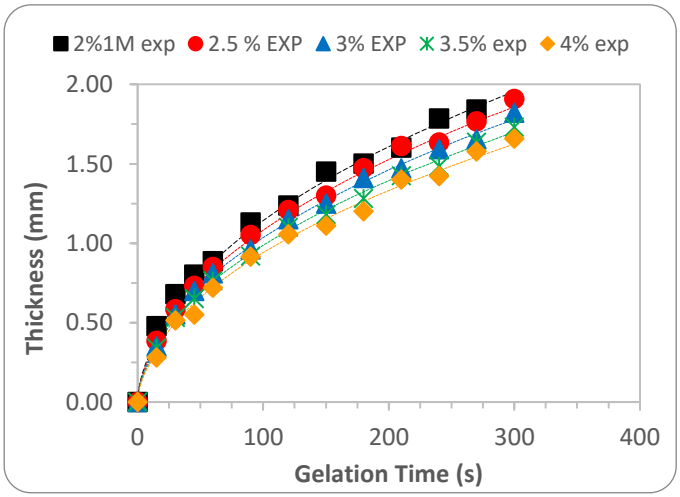

Figure 5.4. Measured and calculated increase of hydrogel thickness as a function of gelation time (for different chitosan concentrations; symbols - measured values; solid lines - calculated values (NaOH solution **4M**). The legend gives the polymer concentration (in wt %).

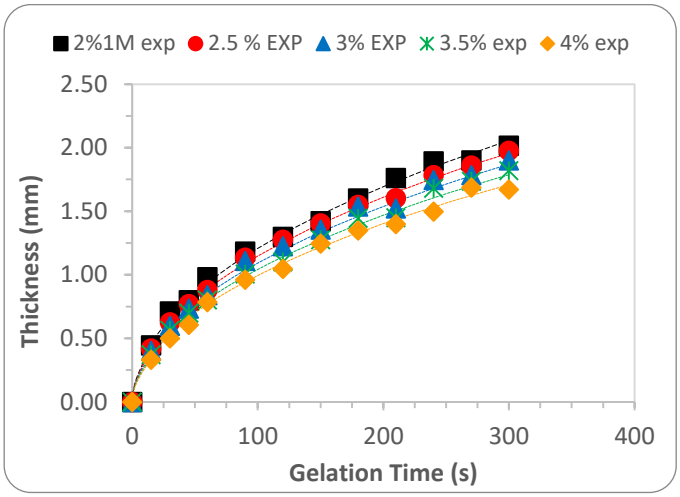

Figure 5.5. Measured and calculated increase of hydrogel thickness as a function of gelation time for different chitosan concentrations; symbols-measured values; solid lines- calculated values (NaOH solution **7M**). The legend gives the polymer concentration (in wt %).

5.1.2 Modeling of the chitosan coagulation process in cylindrical geometry

5.1.2.1 Mathematical model

In order to obtain a mathematical model of the coagulation process, the following hypothesis were adopted: (1) the neutralization reaction between the $-NH_3^+$ groups and NaOH is instantaneous (Knaul, 1997), so that the step controlling the coagulation kinetics is the diffusion of NaOH trough the gel; (2) the NaOH concentration at the gel / chitosan solution interface is negligible small; (3) the concentration of sodium hydroxide inside the chitosan solution is null; (4) the NaOH concentration in coagulation solution is approximated constant in time. This hypothesis is supported by the very high excess of NaOH into the aqueous solution; (5) the NaOH diffusion coefficient is constant inside chitosan hydrogel.

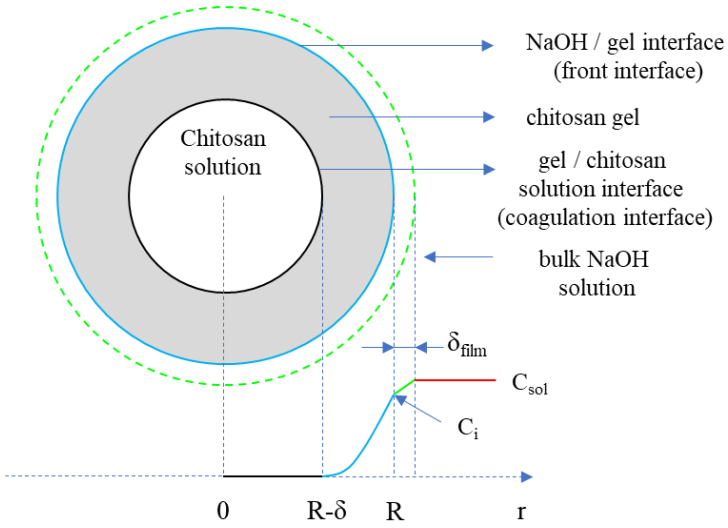

Figure 5.6. The chitosan gel formation in cylindrical geometry coagulation

The sodium hydroxide balance inside the chitosan gel is given by Fick's second law expression:

$$(1-\varepsilon)\frac{\partial C}{\partial t} = \frac{1}{r}\frac{\partial}{\partial r}\left(rD_{ef}\frac{\partial C}{\partial r}\right) \quad \textbf{(5.1)}$$

with the initial condition:

- **t = 0, 0 ≤ r ≤ R,** $C(r,0) = 0$ **(5.2)**

and the boundary conditions (Figure 5.6):

- **t = 0, r = R,** $k_L\left(C_{sol} - C_i\right) = D_{ef}\frac{\partial C}{\partial r}$ **(5.3)**
- **t > 0, r = R – δ,** $C(r,t) = 0$ **(5.4)**

The time evolution of gel thickness is calculated considering the stoichiometric relationship between the molar fluxes of NaOH and $–NH_3^+$ groups consumed at the coagulation interface, r=R-δ, defined by the equation:

- **t > 0, r = R – δ,** $D_{ef}\frac{\partial C(r,t)}{\partial r} = \frac{\partial \delta}{\partial t}C_p n_{NH_2}$ **(5.5)**

In the above equations:

D_{ef} - diffusion coefficient of NaOH through the chitosan hydrogel; C - NaOH concentration in hydrogel; C_{sol} - NaOH concentration in bulk NaOH solution; C_i -NaOH concentration in liquid on the gel-solution interface; C_p - chitosan concentration in chitosan solution; K- NaOH partition coefficient; n_{NH2} - the number of $–NH_3^+$ groups/mole chitosan; ε – solid fraction; δ - the hydrogel thickness.

The only parameter of these equations is the effective sodium hydroxide diffusion coefficient inside the chitosan hydrogel, D_{ef}, because the mass transfer coefficient was determined using the relation proposed by Geankoplis (1993).

According to Geankoplis (1993), the mass transfer coefficient can be calculated using the equation (5.18):

$$J_D = 0.6\,\mathrm{Re}^{-0.487} \quad \textbf{(5.18)}$$

5.1.2.2 Process simulation and calculation of the diffusion coefficient

In our previous investigations, we identified values of NaOH diffusion coefficients in the chitosan gel, between 10^{-9} and $1.85\cdot10^{-9}$ m^2/s. Starting from these results, we selected the values of the diffusion coefficient corresponding to the best fit of experimental points for each pair of chitosan and sodium hydroxide concentrations. The results for different chitosan and NaOH concentrations are presented in Table 5.1. All these values were calculated using a mass transfer coefficient value, $k_L=1.88\cdot10^{-5}$ m/s, obtained by using the equations presented above.

The diffusion coefficient values presented in Table 5.1 are evidencing a small decrease of sodium hydroxide diffusivity in the hydrogel, with the increase of chitosan concentration, presumably due to higher obstructions generated by the increase of solid volume fraction in the gel. In the same

time, it was observed a decrease of diffusion coefficient with the increase of sodium hydroxide concentration from 1 M to 7 M, probably due to the increase of solution viscosity.

Table 5.1. Calculated diffusion coefficient values

Chitosan concentration, (wt %)		**2.00**	**2.50**	**3.00**	**3.50**	**4.00**
$D_{ef} \cdot 10^9$, m^2/s	**1M**	1.10	1.05	1.00	0.95	0.90
	4M	1.05	1.00	0.95	0.90	0.85
	7M	1.00	0.95	0.90	0.85	0.80

The results presented in Figure 5.3, 5.4 and 5.5 are evidencing a good agreement between the calculated and experimental hydrogel thickness values on all the working domain, demonstrating the adequacy of the proposed mathematical model. As expected, as in the case of linear diffusion, the increase of the gel thickness is faster on the first part of coagulation process, due to the smaller diffusion distance of coagulant between the front interface and the coagulation interface. At longer gelation times, the transport distance inside the gel is larger and the growth rate of the hydrogel is decreasing, becoming almost constant at the end of the coagulation process, where the curves have approximately linear shapes.

Several values of diffusion coefficients, calculated from linear and radial coagulation experiments, in identical working conditions, are given in Table 5.2. As observed, the diffusion coefficient values estimated from radial (cylindrical) coagulation experiments, are smaller, the differences between the two sets of values amounting between 35 and 40 %. Similar results were reported by Hermans (1947) in one of the pioneering studies of diffusion-reaction processes with mobile boundary, and confirmed later on by Liu (Liu et al., 1989).

These differences are believed to occur due to the particularities of the diffusion transport in the radial (cylindrical) coagulation, where the transport surface area is continuously shrinking. Additionally, in the case of chitosan coagulation, the structural heterogeneity evidenced in paragraph 4.3.1 (Figure 4.3), could also be a factor accenting the difference between the rates of linear and radial diffusion. The denser zone of the gel has a higher volume fraction in the case of radial diffusion, this slowing the coagulation rate and leading to lower effective diffusion coefficients.

Table 5.2. Comparison of diffusion coefficient values calculated from linear and cylindrical (radial) coagulation data ($10^9 \cdot$Def, m^2/s).

Chitosan conc. (wt %)	**2 %**	**2.5 %**	**2.8 %**	**3.3 %**	**3.9 %**
NaOH solution 1M					
Linear	1.7	1.65	1.55	1.50	1.45
Cylindrical	1.10	1.05	1.10	0.95	0.90
NaOH solution 7M					
Linear	1.55	1.50	1.45	1.40	1.35
Cylindrical	1.0	0. 95	0.90	0.85	0.80

These results are suggesting that in the accurate calculation of the wet spinning processes, there should be used diffusion coefficient values determined from experiments conducted in cylindrical coagulation systems.

5.2 Mathematical modelling of chitosan wet spinning process

5.2.1 The wet spinning laboratory plant

The aim of this study was to investigate, mainly from modelling point of view, the process of chitosan fibers formation by coagulation from aqueous solution using sodium hydroxide solution as coagulant (wet spinning). The experimental data were obtained using a spinning plant existing at the Laboratory "Ingénierie des Matériaux Polymères" (LIMP), University Claude Bernard Lyon. An overview of the plant is presented in Figure 5.8.

Figure 5.8. Chitosan spinning plant overview.

The main components of the spinning plant are **the injection module**, **the coagulation module**, **the washing module** (two baths connected in series), **the drying module** *(*fans and furnace*)* and **the spooling module**. The plant is provided with instrumentation and control devices, connected to *the control panel*. The structural scheme of the spinning plant is shown in Figure 5.9. The dimensions of the coagulation bath and the washing baths are 150 cm length, 20 cm height and 13 cm width. At the output of coagulation bath, a pulling roller system serves to draw the fiber from the bath.

The aim of this study was to investigate only the coagulation step of the wet spinning process. Consequently, the experiments were stopped when the fiber leaved the coagulation bath, so the other components of the plant (washer module, drying module and spooling system) were not used. The concentration of the dope chitosan solution was 2.5 % (w/w) and the NaOH solution volume was close to 40 L and 1.5 M concentration. The fiber was drawn by a pulling roller with constant velocity of 300 rph. The diameter of the roller was 6 cm. The coagulation time (the residence time of the fiber in the coagulation bath) was varied by modifying the fiber path inside the bath (as illustrated in Figure 5**.**10). The samples were taken in the point where the thread was leaving the coagulation bath, by cutting the cylinder with a scissor. Further, the non-coagulate chitosan solution from the sample was removed by using the compressed air. Finally, the chitosan thickness was measured using a microscope Olympus BX41, coupled with Olympus DP26 camera connected on-line at a PC.

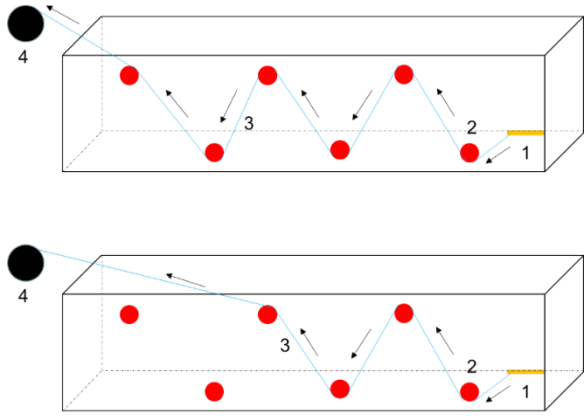

Figure 5.10. Different fiber paths used to vary the coagulation time: (1) spinneret; (2) roll; (3) chitosan fiber; (4) pulling roller. The arrows indicate the displacement direction of the fiber.

5.2.2 Mathematical model of the fiber formation by chitosan coagulation

The mathematical model used was the same as the model used for the study of the chitosan coagulation in cylindrical geometry (equations 5.8, 5.2, 5.3, 5.4 and 5.5), where the coagulation time was considered equal to the residence time in the bath.

The mass transfer coefficient of NaOH between the liquid and the chitosan fiber was determined using the Rotte correlation (Rotte et al., 1969). This correlation was obtained from mass transfer experiments occurring between a liquid and a continuous wire of nickel passing through a vertical recipient filled with $Fe(CN)_2$. As characteristic length in the definitions of the Sh and Pe number was chosen the height of the liquid in the recipient. The experimental data were correlated as the dependence betweeen Sherwood number and the square root of Peclet number given by the equation 5.24:

$$Sh = 1.13\sqrt{Pe} \quad for \quad 4\cdot10^3 < \sqrt{Pe} < 4\cdot10^4 \quad and \quad Sc > 700 \qquad \textbf{(5.24)}$$

$$Pe = \frac{UL}{D};\ Sh = \frac{k_L L}{D} \qquad \textbf{(5.25)}$$

U - fiber velocity; L - characteristic length (in our case is the distance between two pulling rollers in the coagulation bath (~ 20 cm), see the Figure 5.11; D - diffusion coefficient of NaOH in liquid; k_L- mass transfer coefficient;

The diffusion coefficient of the sodium hydroxide in liquid was considered $1.83\cdot10^{-9}$ m^2/s (see the paragraph 4.3.2).

5.2.3 Results and conclusion

The solutions of the equations (5.8) and (5.5) were obtained by the numerical method described in the paragraph 5.1.2.2. The coagulation time, i.e. the residence time of the fiber in the bath was calculated from the length of its trajectory and the rotation speed of the pooling roller. The length of the fiber trajectory was measured using a twine, at the end of the experiments. The gel thickness obtained in coagulation bath was measured, following the same procedure as in the experiments described in the paragraph 5.1.1.1 using a microscope Olympus BX41. The results are presented in Table 5.3.

The effective NaOH diffusion coefficient inside the chitosan hydrogel, D_{ef}, used in the calculations, was calculated by interpolation of the values presented in Table 5.1 and was approximately $1.04 \cdot 10^{-9}$ m^2/s. This was necessary, because the NaOH concentration in the coagulating solution used in the spinning plant (1.5 M) is intermediary between those considered in the radial diffusion experiments.

The value of the mass transfer coefficient, calculated from the relations (5.24) and (5.25) was approximately $1.49 \cdot 10^{-5}$ m/s.

The experimental data (the points) and the theoretical curves (solid lines) are comparatively presented in Fig. 5.12, where the theoretical line was obtained for the diffusion coefficient value, $D_{ef}=1.04 \cdot 10^{-9}$ m^2/s. As seen from this figure, the proposed coagulation model fits satisfactorily the experimental data.

Table 5.3. Results from spinning plant.

Sample number	Fiber length, (cm)	Rotation speed, (rot/h)	Rotation speed, (rot/s)	Length for one rotation, (cm/rot)	Residence time, (s)	Experimental thickness, (mm)
1	55	300	0.0833	18.84	35	0.600
2	100	300	0.0833	18.84	64	0.650
3	127	300	0.0833	18.84	81	0.720
4	150	300	0.0833	18.84	96	0.900
5	166	300	0.0833	18.84	106	0.840
6	180	300	0.0833	18.84	115	1.050

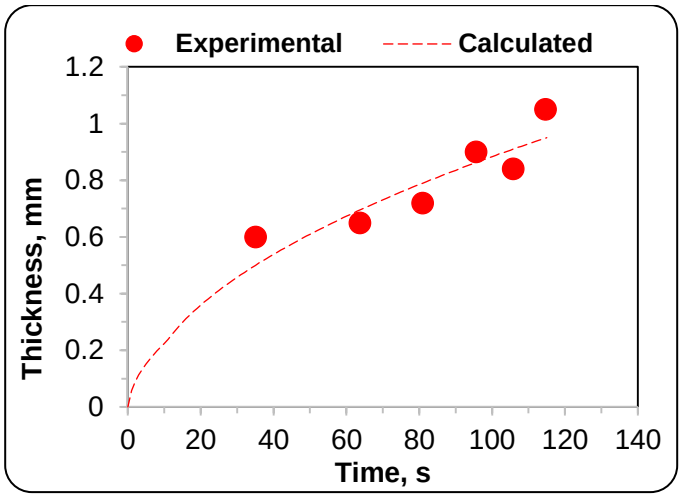

Figure 5.12. Measured and calculated hydrogel thickness in time, for 2.5% chitosan and 1.5M NaOH solution; ● - radial diffusion, samples tacked from spinning plant and measured under microscope; solid lines - calculated values using radial diffusion model ($D_{ef}=1.04 \cdot 10^{-9}$ m^2/s).

The NaOH concentration profiles, inside the hydrogel, calculated at different coagulation times, are given in Figure 5.13. The NaOH concentration at the front interface is not constant, showing an increasing evolution in time, due the increasing of the gel resistance to the NaOH transport toward the coagulation interface, as result of the gel thickness increase. The increasing resistance of the gel thickness is inducing a decrease of NaOH flux and an increased NaOH concentration in the gel volume.

The modelling and simulation study of the chitosan hydrogel wet-spinning described in this paragraph, evidenced an acceptable agreement between the calculated and the measured data on a laboratory wet-spinning unit. This is proving that the proposed model, based on the Second Fick Law, associated to the hypothesis of instantaneous reaction between the NaOH and chitosan $-NH_3^+$ moieties is adequate in the calculation of fiber coagulation step of the wet-spinning process.

GENERAL CONCLUSIONS

The chitosan is a biomaterial that has been proved to be very useful in practical applications, so that its processing, properties and utilizations are the subject of a large number of published studies. Among the chitosan physical states used in practice, the hydrogels present a particular importance. These are usually prepared by coagulation of aqueous chitosan solutions. The experimental studies evidenced that, among the factors influencing the hydrogel properties, an important one is the coagulation kinetics.

In spite of its importance, the number of publications investigating the coagulant transport in chitosan hydrogels is relatively low. The present work brings some contributions to the enrichment of data regarding the engineering process of chitosan hydrogels and chitosan fibers manufacturing.

The principal conclusions of the experimental and theoretical investigations described in the previous chapters are the following:

1) The rheological study of chitosan hydrogels evidenced that the hydrogel hardness increases with the increase of the chitosan concentration and with the increase of the sodium hydroxide concentration. This involves that two chitosan hydrogels, obtained in the same conditions but containing different polymer mass fractions, will have different resistances to mass transport by diffusion (in particular, different values of the coagulant diffusion coefficient, during coagulation process).

2) The hydrogel structure images obtained by confocal laser scanning microscopy and scanning electron microscopy highlighted the appearance of some microstructure with non-homogeneities inside the hydrogels in the diffusion direction. These microstructures are influencing the diffusion properties of the hydrogel. The gel zone in the vicinity of the surface in contact with the sodium hydroxide (front interface) is denser and opposes a higher resistance to diffusion, as compared with the gel zone in the neighborhood of (ending) gel surface in contact with chitosan (dope) solution (coagulation interface). Therefore, the value of the coagulant diffusion coefficient is variable across the gel thickness and is expected to increase, during the coagulation process, from the front interface toward the coagulation interface.

3) A first set of NaOH diffusion coefficient values were determined from experiments consisting in the NaOH release from gel samples impregnated with different concentrations of sodium hydroxide, immersed in a volume of distilled water under stirring. The diffusion NaOH coefficient in the gel was calculated from the measured time evolution of NaOH concentration released from the gel (by the intermediate of the measured pH of the solution).

Nevertheless, the quality of the obtained results is rather modest, these presenting a significant dispersion and a poor reproducibility. These is explained by several factors: the experimental error in the measurement of the pH, the unsteady character of the process, the limited mixing of the liquid, the non-homogeneities occurring in the gel structure appearing during the coagulation process (see chapter 2), the possible changes in the gel structure during the interval between their preparation and their use in experiments, the errors in the measurement of disk thickness, the changes in the NaOH

concentration in the solution due to the absorption of carbon dioxide from air etc. These results were considered rather uncertain, so more accurate methods were adopted, based on the kinetics of chitosan coagulation process.

4) A second set of experiments used in the determination of coagulant diffusion coefficient were performed by a more accurate method, using a parallelepiped shaped, transparent diffusion cell and an optical microscope provided with on-line computer interface. By coagulation experiments with the coagulant transport along the cell (linear diffusion), several important kinetic specificities of the chitosan coagulation from acid aqueous solutions were evidenced. The coagulation kinetics (displacement speed of the coagulation front) was found to be faster at lower chitosan concentrations and higher coagulation agent (base) concentrations.

5) The decrease of the coagulation front speed with the increase of chitosan concentration is explained by the increased number of NH_3^+ moieties to be neutralized, combined with a slightly higher resistance opposed by solid phase to coagulant diffusion (lower value of *NaOH* diffusion coefficient in the gel). However, the dependence of coagulation front speed on chitosan concentration is not linear. At a given coagulation agent concentration and coagulation time, the ratio of the gel thicknesses obtained for two chitosan concentrations is smaller than the reversed chitosan concentrations ratio.

6) The effect of *NaOH* concentration growth in the solution used as coagulation agent, from *1M* to *7M*, keeping the chitosan concentration constant at 1 %, is a significant increase of mass flux on the front interface and a less important increase of the flux on the coagulation interface. The flux on the coagulation interface, when using *NaOH* solution *7M*, is only slightly superior to that corresponding to the solution *1M*, thus explaining the value of gel thickness, not very different of that obtained with the coagulant concentration *1M*. The difference between the NaOH fluxes on the two hydrogel extremities appears due to the amount of *NaOH* accumulated inside the gel, which is superior to the amount consumed in the coagulation reaction, the ratio between the two quantities rising with the *NaOH* concentration in the solution used for coagulation.
All these observations occur as consequence of the controlling effect of the coagulant transport in the gel, toward the coagulation interface, on the overall process kinetics.

7) The experimental data evidenced that the increase of the gel thickness is faster on the first interval of coagulation process, due to the smaller diffusion distance of coagulant between the front interface and the coagulation interface. At longer coagulation times, the transport distance inside the gel is larger, the resistance opposed to coagulant transport increases and the growth rate of the hydrogel is decreasing, becoming almost constant at the end of the coagulation process, where the curves have approximately linear shapes.

8) The modeling and simulation studies confirmed that the chitosan coagulation process is adequately described by the second law of Fick, associated with the hypothesis of instantaneous reaction between NaOH and NH_3^+ groups of the chitosan chains in the dope. The proposed mathematical model of the coagulation process includes the resistances to the NaOH transport, appearing both in the liquid phase (NaOH solution) at the gel vicinity and inside the growing hydrogel stratus.

9) The parameter estimation studies, together with *pH* measurements performed in immerged *NaOH* aqueous solutions inside the prepared hydrogels, indicated that the *NaOH* partition coefficient, K, between *NaOH* solution and chitosan hydrogel is close to unity, so in this modeling and simulation study the value K=1 was assumed. This is in agreement with the theoretical interpretation of the partition coefficient for non-adsorbed solutes and was supported by a weak sensitivity of the gel

thickness evolution in respect with K, in the vicinity of the value K=1, evidenced by process simulations.

10) The obtained NaOH diffusion coefficient values in the chitosan gel are in an acceptable agreement with published data and the theoretical predictions by published correlations. Constructing the graphs diffusion coefficient - chitosan concentration and extrapolating to null chitosan concentration, there were obtained the values 1.9 10^{-9} m^2 s^{-1} for the solution *1M* and 1.76 10^{-9} m^2 s^{-1} for the 7*M* solution. These are in a reasonable agreement with the value of the *NaOH* diffusion coefficient in the solution *1M* reported in literature ($1.75 \cdot 10^{-9}$ m^2/s) and the one estimated from published values of ions diffusivities ($2.125 \cdot 10^{-9}$ m^2/s).

11) Among the published relations proposed for the estimation of the diffusion coefficients in the gels, based on the obstruction theory, the most appropriate for the NaOH diffusion in chitosan hydrogel, proved to be the one formulated by Mackie and Mears, which is approaching our data with a difference between 8 and 9 %.

12) The study of the chitosan coagulation in cylindrical geometry (radial diffusion of sodium hydroxide) evidenced that diffusion coefficient values determined from radial coagulation experiments are lower than those obtained from linear coagulation, a result reported also by other authors. We believe that this occurs due to combined influences of transport geometry and structural non-homogeneity of chitosan gel, evidenced experimentally. Thus, in the calculations of the cylindrical coagulation, it is recommended to use diffusion coefficient values obtained from specific experiments performed with systems having the same geometry.

13) The modelling and simulation study of the chitosan hydrogel wet-spinning conducted to results in an acceptable concordance with the measured data on a laboratory unit. This is proving that the proposed model can be used in the calculation of the coagulation step of the fiber formation process by wet spinning.

REFERENCES (SELECTION)

Amsden B., (**1998b**), Solute Diffusion within Hydrogels. Mechanisms and Models, Macromolecules, vol. 31, pp. 8382-8395.

Anitha A., Sowmya S., Kumar S.P.T., Deepthi S., Chennazhi K.P., Ehrlich H., Tsurkan M., Jayakumar R., (**2014**), Chitin and chitosan in selected biomedical applications, Progress in Polymer Science, vol. 39, Issue 9, pp. 1644-1667.

Bernkop-Schnürch A., Dünnhaupt S., (**2012**), Chitosan-based drug delivery systems, Eur. J. Pharm. Biopharm., vol. 81, pp. 463–469.

Bird R. B., Stewart W. E., Lightfoot E. N., (**2002**), Transport Phenomena, John Wiley & Sons, p. 686

Crank J., (**1975**), The Mathematics of Diffusion, 2nd, New York, ed. Oxford: Clarendon Press.

Croisier F., Jerome C., (**2013**), Chitosan-based biomaterials for tissue engineering, Eur. Polym. J., vol. 49, pp. 780–792.

Cussler E.L., (**1997**), Diffusion, Mass Transfer in Fluids Systems, 2nd ed., Cambridge, Cambridge University Press, p.162, 166 and 237.

Geankoplis C. J., (**1993**), Transport Processes and Unit Operations, 3rd Edition, New Jersey, Prentice-Hall Englewood Cliffs, pag 450.

Hermans J. J., (**1947**), Diffusion with Discontinuous Boundary, Journal of Colloid Science, vol. 2 (4), pp. 387–398.

Kiusalaas J., (**2005**), Numerical Methods in Engineering with Matlab, Cambridge, Cambridge University Press.

Kishida A., Ikada Y., (**2002**), Hydrogels for biomedical and pharmaceutical applications, In Dumitriu, S., Ed, Polymeric biomaterials, 2nd, New York, CRC Press, pp 133-145.

Knaul J. Z., Creber K A. M., (**1997**), Coagulation Rate Studies of Spinnable Chitosan Solutions, Journal of Applied Polymer Science, vol. pp. 66, 117–127.

Lauffer M. A., (**1961**), Theory of Diffusion in Gels, Biophys J., vol. 1, pp. 205-213.

Lee S. H., (**2000**), The mechanism and characteristics of dry-jet wet spinning of chitosan fibers, Journal of the Korean Fiber Society, vol. 37, pp. 374-381.

Li C., Han Q., Guan Y., Zhang Y., (**2014**), Thermal gelation of chitosan in an aqueous alkali-urea solution, Soft Matter, vol. 10, pp. 8245–8253.

Liu C. K., Cuculo J. A., Smith B., (**1989**), Coagulation Studies for Cellulose in the Ammonia / Ammonium Thiocyanate (NH3 / NH4SCN) Direct Solvent System, J. Polym. Sci. Polym. Phys. Part B., vol. 27 (12), pp. 2493-2511.

Massaro L., Zhu X.X., (**1999**), Physical models of diffusion for polymer solutions, gels and solids, Prog. Polym. Sci., vol. 24, pp. 731–775.

Mohammad F., (**2013**), Green Chemistry Approaches to Develop Antimicrobial Textiles Based on Sustainable Biopolymers-A Review, Ind. Eng. Res., vol. 52, pp. 5245–5260.

Nie J. et al., (**2015**), Orientation in multi-layer chitosan: morphology, mechanism and design principle, Sci. Rep., vol. 5, pp. 1-7.

Nie J., Wang Z., Hu Q., (**2016**), Difference between Chitosan Hydrogels via Alkaline and Acidic Solvent Systems, Scientific Reports.

Rotte J. W., Tummers G. L. J., Dekker J. L., (**1969**), Mass transfer to a moving continuous cylinder, Chemical Engineering Science, vol. 24, pp. 1009-1015.

Schatz C., Lucas J. M., Viton C., Domard A., Picho, C., Delair T., (**2004**), Formation and Properties of Positively Charged Colloids Based on Polyelectrolyte Complexes of Biopolymers, Langmuir, vol. 20, pp. 7766-7778.

Venault A., Bouyer D., Pochat-Bohatier C., Vachoud L., Faur C., (**2012**), Investigation of chitosan gelation mechanisms by a modeling approach coupled to local experimental measurement, AIChE J., vol. 58, pp. 2226-2240

Zhang H., Li Y., Zhang X., Liu B., Zhao H., et al., (**2016**) Directly determining the molecular weight of chitosanwith atomic force microscopy, Front Nanosci Nanotech, vol. 2 (3), pp. 123-127.

LIST OF PUBLISHED WORKS

- **Enache A. A.**, David L., Puaux J.-P., Banu I., Bozga G., "Kinetics of chitosan coagulation from aqueous solutions", in *Journal of Applied Polymer Science*, vol. 135, no. 16, 2018, DOI:10.1002/app.46062, Impact Factor: 1.86.

- Sereni N., **Enache A**. **A.**, Sudre G., Montembault A., Rochas C., Durand P., Perrard M.H., Bozga G., Puaux J.-P., Delair T., David L., (**2017**). „Dynamic structuration of physical chitosan hydrogels", *Langmuir*, vol. 33 (44), pp 12697–12707, Impact Factor: 3.833.

- **Enache A. A.**, David L., Puaux J.-P., Banu I., Bozga G., (**2018**), „A modelling study of chitosan wet spinning process", *UPB Scientific Bulletin, Series B*, In curs de publicare.

- **Enache A**.**A.**, David L., Puaux J.-P, Banu I., Bozga G., "A Kinetic Study of Chitosan Coagulation from Aqueous Solutions"**,** *Conferinta RICCCE 20*, Poiana Brasov, Sept. 2017.